

The International Association for the Properties of Water and Steam

Erlangen, Germany

September 1997

Release on the IAPWS Industrial Formulation 1997 for the Thermodynamic Properties of Water and Steam

©1997 International Association for the Properties of Water and Steam
Publication in whole or in part is allowed in all countries provided that attribution is given to the
International Association for the Properties of Water and Steam

President:

Dr. R. Fernández-Prini
Comisión Nacional de Energía Atómica
Av. Libertador 8250
Buenos Aires - 1429
Argentina

Executive Secretary:

Dr. R. B. Dooley
Electric Power Research Institute
3412 Hillview Avenue
Palo Alto, California 94304, USA

This release contains 48 numbered pages.

This release has been authorized by the International Association for the Properties of Water and Steam (IAPWS) at its meeting in Erlangen, Germany, 14-20 September 1997, for issue by its Secretariat. The members of IAPWS are Argentina, Canada, the Czech Republic, Denmark, Germany, France, Italy, Japan, Russia, the United Kingdom, and the United States of America.

The formulation provided in this release is recommended for industrial use, and is called "IAPWS Industrial Formulation 1997 for the Thermodynamic Properties of Water and Steam" abbreviated to "IAPWS Industrial Formulation 1997" (IAPWS-IF97). The IAPWS-IF97 replaces the previous industrial formulation "The 1967 IFC-Formulation for Industrial Use" (IFC-67) [1]. Further details about the formulation can be found in the corresponding article by W. Wagner et al. [2].

IAPWS also has a formulation intended for general and scientific use.

Further information about this release and other documents issued by IAPWS can be obtained from the Executive Secretary of IAPWS.

Contents

1 Nomenclature	3
2 Structure of the Formulation	4
3 Reference Constants	5
4 Auxiliary Equation for the Boundary between Regions 2 and 3	5
5 Equations for Region 1	6
5.1 Basic Equation	6
5.2 Backward Equations	9
5.2.1 The Backward Equation $T(p,h)$	10
5.2.2 The Backward Equation $T(p,s)$	11
6 Equations for Region 2	12
6.1 Basic Equation	13
6.2 Supplementary Equation for the Metastable-Vapor Region	17
6.3 Backward Equations	20
6.3.1 The Backward Equations $T(p,h)$ for Subregions 2a, 2b, and 2c	22
6.3.2 The Backward Equations $T(p,s)$ for Subregions 2a, 2b, and 2c	26
7 Basic Equation for Region 3	29
8 Equations for Region 4	32
8.1 The Saturation-Pressure Equation (Basic Equation)	33
8.2 The Saturation-Temperature Equation (Backward Equation)	34
9 Basic Equation for Region 5	35
10 Consistency at Region Boundaries	39
10.1 Consistency at Boundaries between Single-Phase Regions	39
10.2 Consistency at the Saturation Line	40
11 Computing Time of IAPWS-IF97 in Relation to IFC-67	42
11.1 Computing-Time Investigations for Regions 1, 2, and 4	42
11.2 Computing-Time Investigations for Regions 3 and 5	44
12 Estimates of Uncertainties	45
13 References	48

1 Nomenclature

Thermodynamic quantities:

c_p	Specific isobaric heat capacity
c_v	Specific isochoric heat capacity
f	Specific Helmholtz free energy
g	Specific Gibbs free energy
h	Specific enthalpy
M	Molar mass
p	Pressure
R	Specific gas constant
R_m	Molar gas constant
s	Specific entropy
T	Absolute temperature ^a
u	Specific internal energy
v	Specific volume
w	Speed of sound
x	General quantity
β	Transformed pressure, Eq. (29a)
γ	Dimensionless Gibbs free energy, $\gamma = g/(RT)$
δ	Reduced density, $\delta = \rho/\rho^*$
Δ	Difference in any quantity
η	Reduced enthalpy, $\eta = h/h^*$
θ	Reduced temperature, $\theta = T/T^*$
ϑ	Transformed temperature, Eq. (29b)
π	Reduced pressure, $\pi = p/p^*$
ρ	Mass density
σ	Reduced entropy, $\sigma = s/s^*$
τ	Inverse reduced temperature, $\tau = T^*/T$
ϕ	Dimensionless Helmholtz free energy, $\phi = f/(RT)$

Superscripts:

o	Ideal-gas part
r	Residual part
*	Reducing quantity
,	Saturated liquid state
„	Saturated vapor state

Subscripts:

c	Critical point
max	Maximum value
RMS	Root-mean-square value
s	Saturation state
t	Triple point
tol	Tolerance of a quantity

Root-mean-square deviation:

$$\Delta x_{\text{RMS}} = \sqrt{\frac{1}{N}(\Delta x)^2},$$

where Δx can be either absolute or percentage difference between the corresponding quantities x ; N is the number of Δx values.

^a Note: T denotes absolute temperature on the International Temperature Scale of 1990.

2 Structure of the Formulation

The IAPWS Industrial Formulation 1997 consists of a set of equations for different regions which cover the following range of validity:

$$\begin{aligned} 273.15 \text{ K} \leq T \leq 1073.15 \text{ K} & \quad p \leq 100 \text{ MPa} \\ 1073.15 \text{ K} < T \leq 2273.15 \text{ K} & \quad p \leq 10 \text{ MPa} . \end{aligned}$$

Figure 1 shows the five regions into which the entire range of validity of IAPWS-IF97 is divided. The boundaries of the regions can be directly taken from Fig.1 except for the boundary between regions 2 and 3; this boundary is defined by the so-called B23-equation given in Section 4. Both regions 1 and 2 are individually covered by a fundamental equation for the specific Gibbs free energy $g(p,T)$, region 3 by a fundamental equation for the specific Helmholtz free energy $f(\rho,T)$, where ρ is the density, and the saturation curve by a saturation-pressure equation $p_s(T)$. The high-temperature region 5 is also covered by a $g(p,T)$ equation. These five equations, shown in rectangular boxes in Fig. 1, form the so-called *basic equations*.

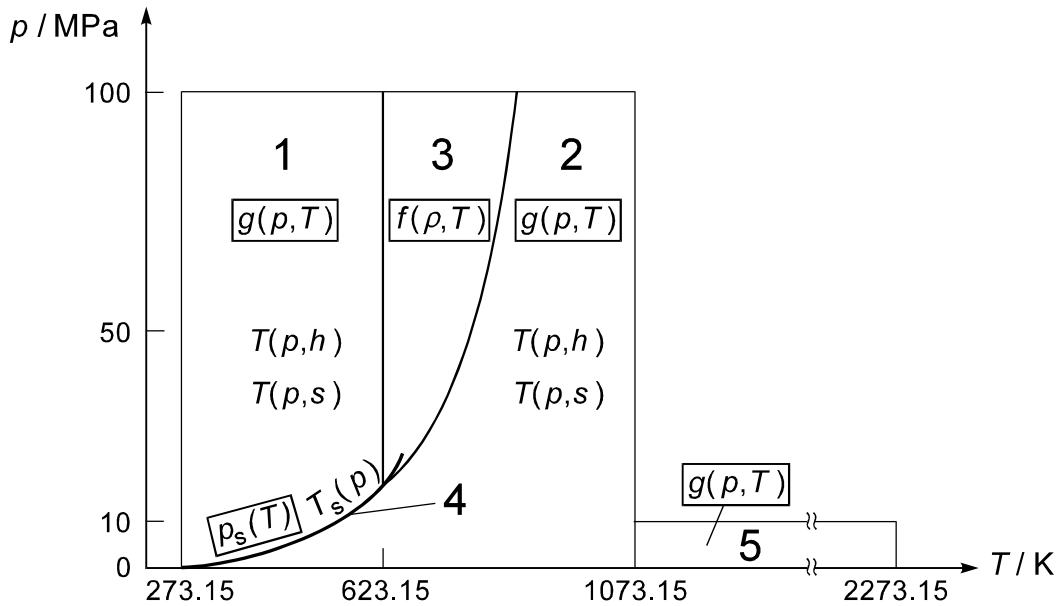


Fig. 1. Regions and equations of IAPWS-IF97.

Regarding the main properties specific volume v , specific enthalpy h , specific isobaric heat capacity c_p , speed of sound w , and saturation pressure p_s , the basic equations represent the corresponding values from the "IAPWS Formulation 1995 for the Thermodynamic Properties of Ordinary Water Substance for General and Scientific Use" [3] (hereafter abbreviated to IAPWS-95) to within the tolerances specified for the development of the corresponding equations; details of these requirements and their fulfillment are given in the comprehensive paper on IAPWS-IF97 [2]. The basic equations for regions 1 and 3 also yield reasonable values for the metastable states close to the stable regions. For region 2 there is a special

equation for the metastable-vapor region. Along the region boundaries the corresponding basic equations are consistent with each other within specified tolerances; for details see Section 10.

In addition to the basic equations, for regions 1, 2, and 4 so-called *backward equations* are provided in form of $T(p,h)$ and $T(p,s)$ for regions 1 and 2, and $T_s(p)$ for region 4. These backward equations are numerically consistent with the corresponding basic equations and make the calculation of properties as functions of p,h and of p,s for regions 1 and 2, and of p for region 4 extremely fast. In this way, properties such as $T(p,h)$, $h(p,s)$, and $h'(p)$ can be calculated without any iteration from the backward equation alone or by combination with the corresponding basic equation, for example, $h(p,s)$ via the relation $h(p,T(p,s))$. As a consequence, the calculation of the industrially most important properties is on average more than five times faster than the corresponding calculation with IFC-67; for details see Section 11.

The estimates of uncertainty of the most relevant properties calculated from the corresponding equations of IAPWS-IF97 are summarized in Section 12.

3 Reference Constants

The specific gas constant of ordinary water used for this formulation is

$$R = 0.461\,526 \text{ kJ kg}^{-1} \text{ K}^{-1}. \quad (1)$$

This value results from the recommended values of the molar gas constant [4], and the molar mass of ordinary water [5, 6]. The values of the critical parameters

$$T_c = 647.096 \text{ K} \quad (2)$$

$$p_c = 22.064 \text{ MPa} \quad (3)$$

$$\rho_c = 322 \text{ kg m}^{-3} \quad (4)$$

are from the corresponding IAPWS release [7].

4 Auxiliary Equation for the Boundary between Regions 2 and 3

The boundary between regions 2 and 3 (see Fig. 1) is defined by the following simple quadratic pressure-temperature relation, the B23-equation

$$\pi = n_1 + n_2\theta + n_3\theta^2, \quad (5)$$

where $\pi = p/p^*$ and $\theta = T/T^*$ with $p^* = 1 \text{ MPa}$ and $T^* = 1 \text{ K}$. The coefficients n_1 to n_3 of Eq. (5) are listed in Table 1. Equation (5) roughly describes an isentropic line; the entropy values along this boundary line are between $s = 5.047 \text{ kJ kg}^{-1} \text{ K}^{-1}$ and $s = 5.261 \text{ kJ kg}^{-1} \text{ K}^{-1}$.

Alternatively Eq. (5) can be expressed explicitly in temperature as

$$\theta = n_4 + [(\pi - n_5) / n_3]^{1/2}, \quad (6)$$

with θ and π defined for Eq. (5) and the coefficients n_3 to n_5 listed in Table 1. Equations (5) and (6) cover the range from 623.15 K at a pressure of 16.5292 MPa to 863.15 K at 100 MPa.

Table 1. Numerical values of the coefficients of the B23-equation, Eqs. (5) and (6), for defining the boundary between regions 2 and 3

i	n_i	i	n_i
1	$0.348\ 051\ 856\ 289\ 69 \times 10^3$	4	$0.572\ 544\ 598\ 627\ 46 \times 10^3$
2	$-0.116\ 718\ 598\ 799\ 75 \times 10^1$	5	$0.139\ 188\ 397\ 788\ 70 \times 10^2$
3	$0.101\ 929\ 700\ 393\ 26 \times 10^{-2}$		

For *computer-program verification*, Eqs. (5) and (6) must meet the following T - p point: $T = 0.623\ 150\ 000 \times 10^3$ K, $p = 0.165\ 291\ 643 \times 10^2$ MPa.

5 Equations for Region 1

This section contains all details relevant for the use of the basic and backward equations of region 1 of IAPWS-IF97. Information about the consistency of the basic equation of this region with the basic equations of regions 3 and 4 along the corresponding region boundaries is summarized in Section 10. The results of computing-time comparisons between IAPWS-IF97 and IFC-67 are given in Section 11. The estimates of uncertainty of the most relevant properties can be found in Section 12.

5.1 Basic Equation

The basic equation for this region is a fundamental equation for the specific Gibbs free energy g . This equation is expressed in dimensionless form, $\gamma = g/(RT)$, and reads

$$\frac{g(p, T)}{RT} = \gamma(\pi, \tau) = \sum_{i=1}^{34} n_i (7.1 - \pi)^{I_i} (\tau - 1.222)^{J_i}, \quad (7)$$

where $\pi = p/p^*$ and $\tau = T^*/T$ with $p^* = 16.53$ MPa and $T^* = 1386$ K; R is given by Eq. (1). The coefficients n_i and exponents I_i and J_i of Eq. (7) are listed in Table 2.

All thermodynamic properties can be derived from Eq. (7) by using the appropriate combinations of the dimensionless Gibbs free energy and its derivatives. Relations between the relevant thermodynamic properties and γ and its derivatives are summarized in Table 3.

All required derivatives of the dimensionless Gibbs free energy are explicitly given in Table 4.

Since the 5th International Conference on the Properties of Steam in London in 1956, the specific internal energy and the specific entropy of the saturated liquid at the triple point have been set equal to zero:

$$u'_t = 0 \quad ; \quad s'_t = 0 . \quad (8)$$

In order to meet this condition at the temperature and pressure of the triple point

$$T_t = 273.16 \text{ K [8]} \quad p_t = 611.657 \text{ Pa [9]} , \quad (9)$$

the coefficients n_3 and n_4 in Eq. (7) have been adjusted accordingly. As a consequence, Eq. (7) yields for the specific enthalpy of the saturated liquid at the triple point

$$h'_t = 0.611 \, 783 \text{ J kg}^{-1} . \quad (10)$$

Table 2. Numerical values of the coefficients and exponents of the dimensionless Gibbs free energy for region 1, Eq. (7)

i	I_i	J_i	n_i	i	I_i	J_i	n_i
1	0	-2	0.146 329 712 131 67	18	2	3	$-0.441 \, 418 \, 453 \, 308 \, 46 \times 10^{-5}$
2	0	-1	-0.845 481 871 691 14	19	2	17	$-0.726 \, 949 \, 962 \, 975 \, 94 \times 10^{-15}$
3	0	0	$-0.375 \, 636 \, 036 \, 720 \, 40 \times 10^1$	20	3	-4	$-0.316 \, 796 \, 448 \, 450 \, 54 \times 10^{-4}$
4	0	1	$0.338 \, 551 \, 691 \, 683 \, 85 \times 10^1$	21	3	0	$-0.282 \, 707 \, 979 \, 853 \, 12 \times 10^{-5}$
5	0	2	-0.957 919 633 878 72	22	3	6	$-0.852 \, 051 \, 281 \, 201 \, 03 \times 10^{-9}$
6	0	3	0.157 720 385 132 28	23	4	-5	$-0.224 \, 252 \, 819 \, 080 \, 00 \times 10^{-5}$
7	0	4	$-0.166 \, 164 \, 171 \, 995 \, 01 \times 10^{-1}$	24	4	-2	$-0.651 \, 712 \, 228 \, 956 \, 01 \times 10^{-6}$
8	0	5	$0.812 \, 146 \, 299 \, 835 \, 68 \times 10^{-3}$	25	4	10	$-0.143 \, 417 \, 299 \, 379 \, 24 \times 10^{-12}$
9	1	-9	$0.283 \, 190 \, 801 \, 238 \, 04 \times 10^{-3}$	26	5	-8	$-0.405 \, 169 \, 968 \, 601 \, 17 \times 10^{-6}$
10	1	-7	$-0.607 \, 063 \, 015 \, 658 \, 74 \times 10^{-3}$	27	8	-11	$-0.127 \, 343 \, 017 \, 416 \, 41 \times 10^{-8}$
11	1	-1	$-0.189 \, 900 \, 682 \, 184 \, 19 \times 10^{-1}$	28	8	-6	$-0.174 \, 248 \, 712 \, 306 \, 34 \times 10^{-9}$
12	1	0	$-0.325 \, 297 \, 487 \, 705 \, 05 \times 10^{-1}$	29	21	-29	$-0.687 \, 621 \, 312 \, 955 \, 31 \times 10^{-18}$
13	1	1	$-0.218 \, 417 \, 171 \, 754 \, 14 \times 10^{-1}$	30	23	-31	$0.144 \, 783 \, 078 \, 285 \, 21 \times 10^{-19}$
14	1	3	$-0.528 \, 383 \, 579 \, 699 \, 30 \times 10^{-4}$	31	29	-38	$0.263 \, 357 \, 816 \, 627 \, 95 \times 10^{-22}$
15	2	-3	$-0.471 \, 843 \, 210 \, 732 \, 67 \times 10^{-3}$	32	30	-39	$-0.119 \, 476 \, 226 \, 400 \, 71 \times 10^{-22}$
16	2	0	$-0.300 \, 017 \, 807 \, 930 \, 26 \times 10^{-3}$	33	31	-40	$0.182 \, 280 \, 945 \, 814 \, 04 \times 10^{-23}$
17	2	1	$0.476 \, 613 \, 939 \, 069 \, 87 \times 10^{-4}$	34	32	-41	$-0.935 \, 370 \, 872 \, 924 \, 58 \times 10^{-25}$

Table 3. Relations of thermodynamic properties to the dimensionless Gibbs free energy γ and its derivatives ^a when using Eq. (7)

Property	Relation
Specific volume $v = (\partial g / \partial p)_T$	$v(\pi, \tau) \frac{p}{RT} = \pi \gamma_\pi$
Specific internal energy $u = g - T(\partial g / \partial T)_p - p(\partial g / \partial p)_T$	$\frac{u(\pi, \tau)}{RT} = \tau \gamma_\tau - \pi \gamma_\pi$
Specific entropy $s = -(\partial g / \partial T)_p$	$\frac{s(\pi, \tau)}{R} = \tau \gamma_\tau - \gamma$
Specific enthalpy $h = g - T(\partial g / \partial T)_p$	$\frac{h(\pi, \tau)}{RT} = \tau \gamma_\tau$
Specific isobaric heat capacity $c_p = (\partial h / \partial T)_p$	$\frac{c_p(\pi, \tau)}{R} = -\tau^2 \gamma_{\tau\tau}$
Specific isochoric heat capacity $c_v = (\partial u / \partial T)_v$	$\frac{c_v(\pi, \tau)}{R} = -\tau^2 \gamma_{\tau\tau} + \frac{(\gamma_\pi - \tau \gamma_{\pi\tau})^2}{\gamma_{\pi\pi}}$
Speed of sound $w = v[-(\partial p / \partial v)_s]^{1/2}$	$\frac{w^2(\pi, \tau)}{RT} = \frac{\gamma_\pi^2}{\tau^2 \gamma_{\tau\tau} - \gamma_{\pi\pi}}$

$$^a \gamma_\pi = \left[\frac{\partial \gamma}{\partial \pi} \right]_\tau, \quad \gamma_{\pi\pi} = \left[\frac{\partial^2 \gamma}{\partial \pi^2} \right]_\tau, \quad \gamma_\tau = \left[\frac{\partial \gamma}{\partial \tau} \right]_\pi, \quad \gamma_{\tau\tau} = \left[\frac{\partial^2 \gamma}{\partial \tau^2} \right]_\pi, \quad \gamma_{\pi\tau} = \left[\frac{\partial^2 \gamma}{\partial \pi \partial \tau} \right]$$

Table 4. The dimensionless Gibbs free energy γ and its derivatives ^a according to Eq. (7)

$$\gamma = \sum_{i=1}^{34} n_i (7.1 - \pi)^{I_i} (\tau - 1.222)^{J_i}$$

$$\gamma_\pi = \sum_{i=1}^{34} -n_i I_i (7.1 - \pi)^{I_i - 1} (\tau - 1.222)^{J_i} \quad \gamma_{\pi\pi} = \sum_{i=1}^{34} n_i I_i (I_i - 1) (7.1 - \pi)^{I_i - 2} (\tau - 1.222)^{J_i}$$

$$\gamma_\tau = \sum_{i=1}^{34} n_i (7.1 - \pi)^{I_i} J_i (\tau - 1.222)^{J_i - 1} \quad \gamma_{\tau\tau} = \sum_{i=1}^{34} n_i (7.1 - \pi)^{I_i} J_i (J_i - 1) (\tau - 1.222)^{J_i - 2}$$

$$\gamma_{\pi\tau} = \sum_{i=1}^{34} -n_i I_i (7.1 - \pi)^{I_i - 1} J_i (\tau - 1.222)^{J_i - 1}$$

$$^a \gamma_\pi = \left[\frac{\partial \gamma}{\partial \pi} \right]_\tau, \quad \gamma_{\pi\pi} = \left[\frac{\partial^2 \gamma}{\partial \pi^2} \right]_\tau, \quad \gamma_\tau = \left[\frac{\partial \gamma}{\partial \tau} \right]_\pi, \quad \gamma_{\tau\tau} = \left[\frac{\partial^2 \gamma}{\partial \tau^2} \right]_\pi, \quad \gamma_{\pi\tau} = \left[\frac{\partial^2 \gamma}{\partial \pi \partial \tau} \right]$$

Range of validity

Equation (7) covers region 1 of IAPWS-IF97 defined by the following range of temperature and pressure; see Fig. 1:

$$273.15 \text{ K} \leq T \leq 623.15 \text{ K} \quad p_s(T) \leq p \leq 100 \text{ MPa} .$$

In addition to the properties in the stable single-phase liquid region, Eq.(7) also yields reasonable values in the metastable superheated-liquid region close to the saturated liquid line.

Note: For temperatures between 273.15 K and 273.16 K at pressures below the melting pressure [10] (metastable states) all values are calculated by extrapolation from Eqs. (7) and (30).

Computer-program verification

To assist the user in computer-program verification of Eq. (7), Table 5 contains test values of the most relevant properties.

Table 5. Thermodynamic property values calculated from Eq. (7) for selected values of T and p ^a

	$T = 300 \text{ K},$ $p = 3 \text{ MPa}$	$T = 300 \text{ K},$ $p = 80 \text{ MPa}$	$T = 500 \text{ K},$ $p = 3 \text{ MPa}$
$v/(\text{m}^3 \text{ kg}^{-1})$	$0.100\ 215\ 168 \times 10^{-2}$	$0.971\ 180\ 894 \times 10^{-3}$	$0.120\ 241\ 800 \times 10^{-2}$
$h/(\text{kJ kg}^{-1})$	$0.115\ 331\ 273 \times 10^3$	$0.184\ 142\ 828 \times 10^3$	$0.975\ 542\ 239 \times 10^3$
$u/(\text{kJ kg}^{-1})$	$0.112\ 324\ 818 \times 10^3$	$0.106\ 448\ 356 \times 10^3$	$0.971\ 934\ 985 \times 10^3$
$s/(\text{kJ kg}^{-1} \text{ K}^{-1})$	0.392 294 792	0.368 563 852	$0.258\ 041\ 912 \times 10^1$
$c_p/(\text{kJ kg}^{-1} \text{ K}^{-1})$	$0.417\ 301\ 218 \times 10^1$	$0.401\ 008\ 987 \times 10^1$	$0.465\ 580\ 682 \times 10^1$
$w/(\text{m s}^{-1})$	$0.150\ 773\ 921 \times 10^4$	$0.163\ 469\ 054 \times 10^4$	$0.124\ 071\ 337 \times 10^4$

^a It is recommended to verify programmed functions using 8 byte real values for all three combinations of T and p given in this table.

5.2 Backward Equations

For the calculation of properties as function of p, h or of p, s without any iteration, the two backward equations require extremely good numerical consistency with the basic equation. The exact requirements for these numerical consistencies were obtained from comprehensive test calculations for several characteristic power cycles. The result of these investigations, namely the assignment of the tolerable numerical inconsistencies between the basic equation, Eq.(7), and the corresponding backward equations, is given in Eqs.(12) and (14), respectively.

5.2.1 The Backward Equation $T(p, h)$

The backward equation $T(p, h)$ for region 1 has the following dimensionless form:

$$\frac{T(p, h)}{T^*} = \theta(\pi, \eta) = \sum_{i=1}^{20} n_i \pi^{I_i} (\eta + 1)^{J_i} , \quad (11)$$

where $\theta = T/T^*$, $\pi = p/p^*$, and $\eta = h/h^*$ with $T^* = 1$ K, $p^* = 1$ MPa, and $h^* = 2500$ kJ kg⁻¹. The coefficients n_i and exponents I_i and J_i of Eq. (11) are listed in Table 6.

Table 6. Numerical values of the coefficients and exponents of the backward equation $T(p, h)$ for region 1, Eq. (11)

i	I_i	J_i	n_i	i	I_i	J_i	n_i
1	0	0	-0.238 724 899 245 21 × 10 ³	11	1	4	-0.659 647 494 236 38 × 10 ¹
2	0	1	0.404 211 886 379 45 × 10 ³	12	1	10	0.939 654 008 783 63 × 10 ⁻²
3	0	2	0.113 497 468 817 18 × 10 ³	13	1	32	0.115 736 475 053 40 × 10 ⁻⁶
4	0	6	-0.584 576 160 480 39 × 10 ¹	14	2	10	-0.258 586 412 820 73 × 10 ⁻⁴
5	0	22	-0.152 854 824 131 40 × 10 ⁻³	15	2	32	-0.406 443 630 847 99 × 10 ⁻⁸
6	0	32	-0.108 667 076 953 77 × 10 ⁻⁵	16	3	10	0.664 561 861 916 35 × 10 ⁻⁷
7	1	0	-0.133 917 448 726 02 × 10 ²	17	3	32	0.806 707 341 030 27 × 10 ⁻¹⁰
8	1	1	0.432 110 391 835 59 × 10 ²	18	4	32	-0.934 777 712 139 47 × 10 ⁻¹²
9	1	2	-0.540 100 671 705 06 × 10 ²	19	5	32	0.582 654 420 206 01 × 10 ⁻¹⁴
10	1	3	0.305 358 922 039 16 × 10 ²	20	6	32	-0.150 201 859 535 03 × 10 ⁻¹⁶

Range of validity

Equation (11) covers the same range of validity as the basic equation, Eq. (7), except for the metastable region (superheated liquid), where Eq. (11) is not valid.

Numerical consistency with the basic equation

For ten million random pairs of p and h covering the entire region 1, the differences ΔT between temperatures from Eq. (11) and from Eq. (7) were calculated and the absolute maximum difference $|\Delta T|_{\max}$ and the root-mean-square difference ΔT_{RMS} were determined. These actual inconsistency values and the tolerated value $|\Delta T|_{\text{tol}}$ (see the beginning of Section 5.2) amount to:

$$|\Delta T|_{\text{tol}} = 25 \text{ mK} ; \quad \Delta T_{\text{RMS}} = 13.4 \text{ mK} ; \quad |\Delta T|_{\max} = 23.6 \text{ mK} . \quad (12)$$

Computer-program verification

To assist the user in computer-program verification of Eq.(11), Table 7 contains the corresponding test values.

Table 7. Temperature values calculated from Eq.(11) for selected values of p and h^a

p/MPa	$h/(\text{kJ kg}^{-1})$	T/K
3	500	$0.391\ 798\ 509 \times 10^3$
80	500	$0.378\ 108\ 626 \times 10^3$
80	1500	$0.611\ 041\ 229 \times 10^3$

^a It is recommended to verify the programmed equation (8 byte real values) for all three combinations of p and h given in this table.

5.2.2 The Backward Equation $T(p, s)$

The backward equation $T(p, s)$ for region 1 has the following dimensionless form:

$$\frac{T(p, s)}{T^*} = \theta(\pi, \sigma) = \sum_{i=1}^{20} n_i \pi^{I_i} (\sigma + 2)^{J_i}, \quad (13)$$

where $\theta = T/T^*$, $\pi = p/p^*$, and $\sigma = s/s^*$ with $T^* = 1\ \text{K}$, $p^* = 1\ \text{MPa}$, and $s^* = 1\ \text{kJ kg}^{-1}\ \text{K}^{-1}$. The coefficients n_i and exponents I_i and J_i of Eq. (13) are listed in Table 8.

Table 8. Numerical values of the coefficients and exponents of the backward equation $T(p, s)$ for region 1, Eq. (13)

i	I_i	J_i	n_i	i	I_i	J_i	n_i
1	0	0	$0.174\ 782\ 680\ 583\ 07 \times 10^3$	11	1	12	$0.356\ 721\ 106\ 073\ 66 \times 10^{-9}$
2	0	1	$0.348\ 069\ 308\ 928\ 73 \times 10^2$	12	1	31	$0.173\ 324\ 969\ 948\ 95 \times 10^{-23}$
3	0	2	$0.652\ 925\ 849\ 784\ 55 \times 10^1$	13	2	0	$0.566\ 089\ 006\ 548\ 37 \times 10^{-3}$
4	0	3	$0.330\ 399\ 817\ 754\ 89$	14	2	1	$-0.326\ 354\ 831\ 397\ 17 \times 10^{-3}$
5	0	11	$-0.192\ 813\ 829\ 231\ 96 \times 10^{-6}$	15	2	2	$0.447\ 782\ 866\ 906\ 32 \times 10^{-4}$
6	0	31	$-0.249\ 091\ 972\ 445\ 73 \times 10^{-22}$	16	2	9	$-0.513\ 221\ 569\ 085\ 07 \times 10^{-9}$
7	1	0	$-0.261\ 076\ 364\ 893\ 32$	17	2	31	$-0.425\ 226\ 570\ 422\ 07 \times 10^{-25}$
8	1	1	$0.225\ 929\ 659\ 815\ 86$	18	3	10	$0.264\ 004\ 413\ 606\ 89 \times 10^{-12}$
9	1	2	$-0.642\ 564\ 633\ 952\ 26 \times 10^{-1}$	19	3	32	$0.781\ 246\ 004\ 597\ 23 \times 10^{-28}$
10	1	3	$0.788\ 762\ 892\ 705\ 26 \times 10^{-2}$	20	4	32	$-0.307\ 321\ 999\ 036\ 68 \times 10^{-30}$

Range of validity

Equation (13) covers the same range of validity as the basic equation, Eq. (7), except for the metastable region (superheated liquid), where Eq. (13) is not valid.

Numerical consistency with the basic equation

For ten million random pairs of p and s covering the entire region 1, the differences ΔT between temperatures from Eq. (13) and from Eq. (7) were calculated and the absolute maximum difference $|\Delta T|_{\max}$ and the root-mean-square difference ΔT_{RMS} were determined. These actual differences and the tolerated value $|\Delta T|_{\text{tol}}$ (see the beginning of Section 5.2) amount to:

$$|\Delta T|_{\text{tol}} = 25 \text{ mK} \quad ; \quad \Delta T_{\text{RMS}} = 5.8 \text{ mK} \quad ; \quad |\Delta T|_{\max} = 21.8 \text{ mK} . \quad (14)$$

Computer-program verification

To assist the user in computer-program verification of Eq. (13), Table 9 contains the corresponding test values.

Table 9. Temperature values calculated from Eq. (13) for selected values of p and s ^a

p/MPa	$s/(\text{kJ kg}^{-1} \text{ K}^{-1})$	T/K
3	0.5	$0.307\,842\,258 \times 10^3$
80	0.5	$0.309\,979\,785 \times 10^3$
80	3	$0.565\,899\,909 \times 10^3$

^a It is recommended to verify the programmed equation using 8 byte real values for all three combinations of p and s given in this table.

6 Equations for Region 2

This section contains all details relevant for the use of the basic and backward equations of region 2 of IAPWS-IF97. Information about the consistency of the basic equation of this region with the basic equations of regions 3, 4 and 5 along the corresponding region boundaries is summarized in Section 10. The auxiliary equation for defining the boundary between regions 2 and 3 is given in Section 4. Section 11 contains the results of computing-time comparisons between IAPWS-IF97 and IFC-67. The estimates of uncertainty of the most relevant properties can be found in Section 12.

6.1 Basic Equation

The basic equation for this region is a fundamental equation for the specific Gibbs free energy g . This equation is expressed in dimensionless form, $\gamma = g/(RT)$, and is separated into two parts, an ideal-gas part γ^o and a residual part γ^r , so that

$$\frac{g(p, T)}{RT} = \gamma(\pi, \tau) = \gamma^o(\pi, \tau) + \gamma^r(\pi, \tau) , \quad (15)$$

where $\pi = p/p^*$ and $\tau = T^*/T$ with R given by Eq. (1).

The equation for the ideal-gas part γ^o of the dimensionless Gibbs free energy reads

$$\gamma^o = \ln \pi + \sum_{i=1}^9 n_i^o \tau^{J_i^o} , \quad (16)$$

where $\pi = p/p^*$ and $\tau = T^*/T$ with $p^* = 1$ MPa and $T^* = 540$ K. The coefficients n_1^o and n_2^o were adjusted in such a way that the values for the specific internal energy and specific entropy in the ideal-gas state relate to Eq. (8). Table 10 contains the coefficients n_i^o and exponents J_i^o of Eq. (16).

Table 10. Numerical values of the coefficients and exponents of the ideal-gas part γ^o of the dimensionless Gibbs free energy for region 2, Eq. (16)^a

i	J_i^o	n_i^o	i	J_i^o	n_i^o
1 ^a	0	$-0.969\,276\,865\,002\,17 \times 10^1$	6	-2	$0.142\,408\,191\,714\,44 \times 10^1$
2 ^a	1	$0.100\,866\,559\,680\,18 \times 10^2$	7	-1	$-0.438\,395\,113\,194\,50 \times 10^1$
3	-5	$-0.560\,879\,112\,830\,20 \times 10^{-2}$	8	2	$-0.284\,086\,324\,607\,72$
4	-4	$0.714\,527\,380\,814\,55 \times 10^{-1}$	9	3	$0.212\,684\,637\,533\,07 \times 10^{-1}$
5	-3	$-0.407\,104\,982\,239\,28$			

^a If Eq. (16) is incorporated into Eq. (18), instead of the values for n_1^o and n_2^o given above, the following values for these two coefficients must be used: $n_1^o = -0.969\,372\,683\,930\,49 \times 10^1$, $n_2^o = 0.100\,872\,759\,700\,06 \times 10^2$.

The form of the residual part γ^r of the dimensionless Gibbs free energy is as follows:

$$\gamma^r = \sum_{i=1}^{43} n_i \pi^{I_i} (\tau - 0.5)^{J_i} , \quad (17)$$

where $\pi = p/p^*$ and $\tau = T^*/T$ with $p^* = 1$ MPa and $T^* = 540$ K. The coefficients n_i and exponents I_i and J_i of Eq. (17) are listed in Table 11.

Table 11. Numerical values of the coefficients and exponents of the residual part γ^r of the dimensionless Gibbs free energy for region 2, Eq. (17)

i	I_i	J_i	n_i
1	1	0	$-0.177\ 317\ 424\ 732\ 13 \times 10^{-2}$
2	1	1	$-0.178\ 348\ 622\ 923\ 58 \times 10^{-1}$
3	1	2	$-0.459\ 960\ 136\ 963\ 65 \times 10^{-1}$
4	1	3	$-0.575\ 812\ 590\ 834\ 32 \times 10^{-1}$
5	1	6	$-0.503\ 252\ 787\ 279\ 30 \times 10^{-1}$
6	2	1	$-0.330\ 326\ 416\ 702\ 03 \times 10^{-4}$
7	2	2	$-0.189\ 489\ 875\ 163\ 15 \times 10^{-3}$
8	2	4	$-0.393\ 927\ 772\ 433\ 55 \times 10^{-2}$
9	2	7	$-0.437\ 972\ 956\ 505\ 73 \times 10^{-1}$
10	2	36	$-0.266\ 745\ 479\ 140\ 87 \times 10^{-4}$
11	3	0	$0.204\ 817\ 376\ 923\ 09 \times 10^{-7}$
12	3	1	$0.438\ 706\ 672\ 844\ 35 \times 10^{-6}$
13	3	3	$-0.322\ 776\ 772\ 385\ 70 \times 10^{-4}$
14	3	6	$-0.150\ 339\ 245\ 421\ 48 \times 10^{-2}$
15	3	35	$-0.406\ 682\ 535\ 626\ 49 \times 10^{-1}$
16	4	1	$-0.788\ 473\ 095\ 593\ 67 \times 10^{-9}$
17	4	2	$0.127\ 907\ 178\ 522\ 85 \times 10^{-7}$
18	4	3	$0.482\ 253\ 727\ 185\ 07 \times 10^{-6}$
19	5	7	$0.229\ 220\ 763\ 376\ 61 \times 10^{-5}$
20	6	3	$-0.167\ 147\ 664\ 510\ 61 \times 10^{-10}$
21	6	16	$-0.211\ 714\ 723\ 213\ 55 \times 10^{-2}$
22	6	35	$-0.238\ 957\ 419\ 341\ 04 \times 10^2$
23	7	0	$-0.590\ 595\ 643\ 242\ 70 \times 10^{-17}$
24	7	11	$-0.126\ 218\ 088\ 991\ 01 \times 10^{-5}$
25	7	25	$-0.389\ 468\ 424\ 357\ 39 \times 10^{-1}$
26	8	8	$0.112\ 562\ 113\ 604\ 59 \times 10^{-10}$
27	8	36	$-0.823\ 113\ 408\ 979\ 98 \times 10^1$
28	9	13	$0.198\ 097\ 128\ 020\ 88 \times 10^{-7}$
29	10	4	$0.104\ 069\ 652\ 101\ 74 \times 10^{-18}$
30	10	10	$-0.102\ 347\ 470\ 959\ 29 \times 10^{-12}$
31	10	14	$-0.100\ 181\ 793\ 795\ 11 \times 10^{-8}$
32	16	29	$-0.808\ 829\ 086\ 469\ 85 \times 10^{-10}$
33	16	50	$0.106\ 930\ 318\ 794\ 09$
34	18	57	$-0.336\ 622\ 505\ 741\ 71$
35	20	20	$0.891\ 858\ 453\ 554\ 21 \times 10^{-24}$
36	20	35	$0.306\ 293\ 168\ 762\ 32 \times 10^{-12}$
37	20	48	$-0.420\ 024\ 676\ 982\ 08 \times 10^{-5}$
38	21	21	$-0.590\ 560\ 296\ 856\ 39 \times 10^{-25}$
39	22	53	$0.378\ 269\ 476\ 134\ 57 \times 10^{-5}$
40	23	39	$-0.127\ 686\ 089\ 346\ 81 \times 10^{-14}$
41	24	26	$0.730\ 876\ 105\ 950\ 61 \times 10^{-28}$
42	24	40	$0.554\ 147\ 153\ 507\ 78 \times 10^{-16}$
43	24	58	$-0.943\ 697\ 072\ 412\ 10 \times 10^{-6}$

All thermodynamic properties can be derived from Eq.(15) by using the appropriate combinations of the ideal-gas part γ^o , Eq.(16), and the residual part γ^r , Eq.(17), of the dimensionless Gibbs free energy and their derivatives. Relations between the relevant thermodynamic properties and γ^o and γ^r and their derivatives are summarized in Table 12. All required derivatives of the ideal-gas part and of the residual part of the dimensionless Gibbs free energy are explicitly given in Table 13 and Table 14, respectively.

Table 12. Relations of thermodynamic properties to the ideal-gas part γ^o and the residual part γ^r of the dimensionless Gibbs free energy and their derivatives ^a when using Eq. (15) or Eq. (18)

Property	Relation
Specific volume $v = (\partial g / \partial p)_T$	$v(\pi, \tau) \frac{P}{RT} = \pi(\gamma_\pi^o + \gamma_\pi^r)$
Specific internal energy $u = g - T(\partial g / \partial T)_p - p(\partial g / \partial p)_T$	$\frac{u(\pi, \tau)}{RT} = \tau(\gamma_\tau^o + \gamma_\tau^r) - \pi(\gamma_\pi^o + \gamma_\pi^r)$
Specific entropy $s = -(\partial g / \partial T)_p$	$\frac{s(\pi, \tau)}{R} = \tau(\gamma_\tau^o + \gamma_\tau^r) - (\gamma^o + \gamma^r)$
Specific enthalpy $h = g - T(\partial g / \partial T)_p$	$\frac{h(\pi, \tau)}{RT} = \tau(\gamma_\tau^o + \gamma_\tau^r)$
Specific isobaric heat capacity $c_p = (\partial h / \partial T)_p$	$\frac{c_p(\pi, \tau)}{R} = -\tau^2(\gamma_{\tau\tau}^o + \gamma_{\tau\tau}^r)$
Specific isochoric heat capacity $c_v = (\partial u / \partial T)_v$	$\frac{c_v(\pi, \tau)}{R} = -\tau^2(\gamma_{\tau\tau}^o + \gamma_{\tau\tau}^r) - \frac{(1 + \pi\gamma_\pi^r - \tau\pi\gamma_{\pi\tau}^r)^2}{1 - \pi^2\gamma_{\pi\pi}^r}$
Speed of sound $w = v[-(\partial p / \partial v)_s]^{1/2}$	$\frac{w^2(\pi, \tau)}{RT} = \frac{1 + 2\pi\gamma_\pi^r + \pi^2\gamma_\pi^{r2}}{(1 - \pi^2\gamma_{\pi\pi}^r) + \frac{(1 + \pi\gamma_\pi^r - \tau\pi\gamma_{\pi\tau}^r)^2}{\tau^2(\gamma_{\tau\tau}^o + \gamma_{\tau\tau}^r)}}$

^a $\gamma_\pi^r = \left[\frac{\partial \gamma^r}{\partial \pi} \right]_\tau$, $\gamma_{\pi\pi}^r = \left[\frac{\partial^2 \gamma^r}{\partial \pi^2} \right]_\tau$, $\gamma_\tau^r = \left[\frac{\partial \gamma^r}{\partial \tau} \right]_\pi$, $\gamma_{\tau\tau}^r = \left[\frac{\partial^2 \gamma^r}{\partial \tau^2} \right]_\pi$, $\gamma_{\pi\tau}^r = \left[\frac{\partial^2 \gamma^r}{\partial \pi \partial \tau} \right]$, $\gamma_\tau^o = \left[\frac{\partial \gamma^o}{\partial \tau} \right]_\pi$, $\gamma_{\tau\tau}^o = \left[\frac{\partial^2 \gamma^o}{\partial \tau^2} \right]_\pi$

Table 13. The ideal-gas part γ^o of the dimensionless Gibbs free energy and its derivatives^a according to Eq. (16)

$$\begin{aligned}
 \gamma^o &= \ln \pi + \sum_{i=1}^9 n_i^o \tau^{J_i^o} \\
 \gamma_{\pi}^o &= 1/\pi + 0 \\
 \gamma_{\pi\pi}^o &= -1/\pi^2 + 0 \\
 \gamma_{\tau}^o &= 0 + \sum_{i=1}^9 n_i^o J_i^o \tau^{J_i^o-1} \\
 \gamma_{\tau\tau}^o &= 0 + \sum_{i=1}^9 n_i^o J_i^o (J_i^o - 1) \tau^{J_i^o-2} \\
 \gamma_{\pi\tau}^o &= 0 + 0
 \end{aligned}$$

$${}^a \gamma_{\pi}^o = \left[\frac{\partial \gamma^o}{\partial \pi} \right]_{\tau}, \gamma_{\pi\pi}^o = \left[\frac{\partial^2 \gamma^o}{\partial \pi^2} \right]_{\tau}, \gamma_{\tau}^o = \left[\frac{\partial \gamma^o}{\partial \tau} \right]_{\pi}, \gamma_{\tau\tau}^o = \left[\frac{\partial^2 \gamma^o}{\partial \tau^2} \right]_{\pi}, \gamma_{\pi\tau}^o = \left[\frac{\partial^2 \gamma^o}{\partial \pi \partial \tau} \right]$$

Table 14. The residual part γ^r of the dimensionless Gibbs free energy and its derivatives^a according to Eq. (17)

$$\begin{aligned}
 \gamma^r &= \sum_{i=1}^{43} n_i \pi^{I_i} (\tau - 0.5)^{J_i} \\
 \gamma_{\pi}^r &= \sum_{i=1}^{43} n_i I_i \pi^{I_i-1} (\tau - 0.5)^{J_i} & \gamma_{\pi\pi}^r &= \sum_{i=1}^{43} n_i I_i (I_i - 1) \pi^{I_i-2} (\tau - 0.5)^{J_i} \\
 \gamma_{\tau}^r &= \sum_{i=1}^{43} n_i \pi^{I_i} J_i (\tau - 0.5)^{J_i-1} & \gamma_{\tau\tau}^r &= \sum_{i=1}^{43} n_i \pi^{I_i} J_i (J_i - 1) (\tau - 0.5)^{J_i-2} \\
 \gamma_{\pi\tau}^r &= \sum_{i=1}^{43} n_i I_i \pi^{I_i-1} J_i (\tau - 0.5)^{J_i-1}
 \end{aligned}$$

$${}^a \gamma_{\pi}^r = \left[\frac{\partial \gamma^r}{\partial \pi} \right]_{\tau}, \gamma_{\pi\pi}^r = \left[\frac{\partial^2 \gamma^r}{\partial \pi^2} \right]_{\tau}, \gamma_{\tau}^r = \left[\frac{\partial \gamma^r}{\partial \tau} \right]_{\pi}, \gamma_{\tau\tau}^r = \left[\frac{\partial^2 \gamma^r}{\partial \tau^2} \right]_{\pi}, \gamma_{\pi\tau}^r = \left[\frac{\partial^2 \gamma^r}{\partial \pi \partial \tau} \right]$$

Range of validity

Equation (15) covers region 2 of IAPWS-IF97 defined by the following range of temperature and pressure, see Fig. 1:

$$\begin{aligned} 273.15 \text{ K} \leq T \leq 623.15 \text{ K} & \quad 0 < p \leq p_s(T)_{\text{Eq.(30)}} \\ 623.15 \text{ K} < T \leq 863.15 \text{ K} & \quad 0 < p \leq p(T)_{\text{Eq.(5)}} \\ 863.15 \text{ K} < T \leq 1073.15 \text{ K} & \quad 0 < p \leq 100 \text{ MPa} \end{aligned}$$

In addition to the properties in the stable single-phase vapor region, Eq. (15) also yields reasonable values in the metastable-vapor region *for pressures above 10 MPa*. Equation (15) is not valid in the metastable-vapor region at pressures $p \leq 10$ MPa; for this part of the metastable-vapor region see Section 6.2.

Note: For temperatures between 273.15 K and 273.16 K at pressures above the sublimation pressure [10] (metastable states) all values are calculated by extrapolation from Eqs. (15) and (30).

Computer-program verification

To assist the user in computer-program verification of Eq. (15), Table 15 contains test values of the most relevant properties.

Table 15. Thermodynamic property values calculated from Eq. (15) for selected values of T and p ^a

	$T = 300 \text{ K},$ $p = 0.0035 \text{ MPa}$	$T = 700 \text{ K},$ $p = 0.0035 \text{ MPa}$	$T = 700 \text{ K},$ $p = 30 \text{ MPa}$
$v/(\text{m}^3 \text{ kg}^{-1})$	$0.394\ 913\ 866 \times 10^2$	$0.923\ 015\ 898 \times 10^2$	$0.542\ 946\ 619 \times 10^{-2}$
$h/(\text{kJ kg}^{-1})$	$0.254\ 991\ 145 \times 10^4$	$0.333\ 568\ 375 \times 10^4$	$0.263\ 149\ 474 \times 10^4$
$u/(\text{kJ kg}^{-1})$	$0.241\ 169\ 160 \times 10^4$	$0.301\ 262\ 819 \times 10^4$	$0.246\ 861\ 076 \times 10^4$
$s/(\text{kJ kg}^{-1} \text{ K}^{-1})$	$0.852\ 238\ 967 \times 10^1$	$0.101\ 749\ 996 \times 10^2$	$0.517\ 540\ 298 \times 10^1$
$c_p/(\text{kJ kg}^{-1} \text{ K}^{-1})$	$0.191\ 300\ 162 \times 10^1$	$0.208\ 141\ 274 \times 10^1$	$0.103\ 505\ 092 \times 10^2$
$w/(\text{m s}^{-1})$	$0.427\ 920\ 172 \times 10^3$	$0.644\ 289\ 068 \times 10^3$	$0.480\ 386\ 523 \times 10^3$

^a It is recommended to verify programmed functions using 8 byte real values for all three combinations of T and p given in this table.

6.2 Supplementary Equation for the Metastable-Vapor Region

As for the basic equation, Eq. (15), the supplementary equation for a part of the metastable-vapor region bounding region 2 is given in the dimensionless form of the specific Gibbs free energy, $\gamma = g/(RT)$, consisting of an ideal-gas part γ^o and a residual part γ^f , so that

$$\frac{g(p, T)}{RT} = \gamma(\pi, \tau) = \gamma^o(\pi, \tau) + \gamma^f(\pi, \tau) , \quad (18)$$

where $\pi = p/p^*$ and $\tau = T^*/T$ with R given by Eq. (1).

The equation for the ideal-gas part γ^o is identical with Eq. (16) except for the values of the two coefficients n_1^o and n_2^o , see Table 10. For the use of Eq. (16) as part of Eq. (18) the coefficients n_1^o and n_2^o were slightly readjusted to meet the high consistency requirement between Eqs. (18) and (15) regarding the properties h and s along the saturated vapor line; see below.

The equation for the residual part γ^r reads

$$\gamma^r = \sum_{i=1}^{13} n_i \pi^{I_i} (\tau - 0.5)^{J_i} , \quad (19)$$

where $\pi = p/p^*$ and $\tau = T^*/T$ with $p^* = 1$ MPa and $T^* = 540$ K. The coefficients n_i and exponents I_i and J_i of Eq. (19) are listed in Table 16.

Note: In the metastable-vapor region there are no experimental data to which an equation can be fitted. Thus, Eq. (18) is only based on input values extrapolated from the stable single-phase region 2. These extrapolations were performed with a special low-density gas equation [11] considered to be more suitable for such extrapolations into the metastable-vapor region than IAPWS-95 [3].

Table 16. Numerical values of the coefficients and exponents of the residual part γ^r of the dimensionless Gibbs free energy for the metastable-vapor region, Eq. (19)

i	I_i	J_i	n_i
1	1	0	$-0.733\ 622\ 601\ 865\ 06 \times 10^{-2}$
2	1	2	$-0.882\ 238\ 319\ 431\ 46 \times 10^{-1}$
3	1	5	$-0.723\ 345\ 552\ 132\ 45 \times 10^{-1}$
4	1	11	$-0.408\ 131\ 785\ 344\ 55 \times 10^{-2}$
5	2	1	$0.200\ 978\ 033\ 802\ 07 \times 10^{-2}$
6	2	7	$-0.530\ 459\ 218\ 986\ 42 \times 10^{-1}$
7	2	16	$-0.761\ 904\ 090\ 869\ 70 \times 10^{-2}$
8	3	4	$-0.634\ 980\ 376\ 573\ 13 \times 10^{-2}$
9	3	16	$-0.860\ 430\ 930\ 285\ 88 \times 10^{-1}$
10	4	7	$0.753\ 215\ 815\ 227\ 70 \times 10^{-2}$
11	4	10	$-0.792\ 383\ 754\ 461\ 39 \times 10^{-2}$
12	5	9	$-0.228\ 881\ 607\ 784\ 47 \times 10^{-3}$
13	5	10	$-0.264\ 565\ 014\ 828\ 10 \times 10^{-2}$

All thermodynamic properties can be derived from Eq. (18) by using the appropriate combinations of the ideal-gas part γ^o , Eq. (16), and the residual part γ^r , Eq. (19), of the dimensionless Gibbs free energy and their derivatives. Relations between the relevant thermodynamic properties and γ^o and γ^r and their derivatives are summarized in Table 12.

All required derivatives of the ideal-gas part and of the residual part of the dimensionless Gibbs free energy are explicitly given in Table 13 and Table 17, respectively.

Table 17. The residual part γ^r of the dimensionless Gibbs free energy and its derivatives^a according to Eq. (19)

$$\gamma^r = \sum_{i=1}^{13} n_i \pi^{I_i} (\tau - 0.5)^{J_i}$$

$$\gamma_{\pi}^r = \sum_{i=1}^{13} n_i I_i \pi^{I_i-1} (\tau - 0.5)^{J_i} \quad \gamma_{\pi\pi}^r = \sum_{i=1}^{13} n_i I_i (I_i - 1) \pi^{I_i-2} (\tau - 0.5)^{J_i}$$

$$\gamma_{\tau}^r = \sum_{i=1}^{13} n_i \pi^{I_i} J_i (\tau - 0.5)^{J_i-1} \quad \gamma_{\tau\tau}^r = \sum_{i=1}^{13} n_i \pi^{I_i} J_i (J_i - 1) (\tau - 0.5)^{J_i-2}$$

$$\gamma_{\pi\tau}^r = \sum_{i=1}^{13} n_i I_i \pi^{I_i-1} J_i (\tau - 0.5)^{J_i-1}$$

$$^a \gamma_{\pi}^r = \left[\frac{\partial \gamma^r}{\partial \pi} \right]_{\tau}, \quad \gamma_{\pi\pi}^r = \left[\frac{\partial^2 \gamma^r}{\partial \pi^2} \right]_{\tau}, \quad \gamma_{\tau}^r = \left[\frac{\partial \gamma^r}{\partial \tau} \right]_{\pi}, \quad \gamma_{\tau\tau}^r = \left[\frac{\partial^2 \gamma^r}{\partial \tau^2} \right]_{\pi}, \quad \gamma_{\pi\tau}^r = \left[\frac{\partial^2 \gamma^r}{\partial \pi \partial \tau} \right]$$

Range of validity

Equation (18) is valid in the metastable-vapor region from the saturated vapor line to the 5 % equilibrium moisture line (determined from the equilibrium h' and h'' values) at pressures from the triple-point pressure, see Eq. (9), up to 10 MPa.

Consistency with the basic equation

The consistency of Eq. (18) with the basic equation, Eq. (15), along the saturated vapor line is characterized by the following maximum inconsistencies regarding the properties v , h , c_p , s , g , and w :

$$\begin{aligned} |\Delta v|_{\max} &= 0.014 \% & |\Delta s|_{\max} &= 0.082 \text{ J kg}^{-1} \text{ K}^{-1} \\ |\Delta h|_{\max} &= 0.043 \text{ kJ kg}^{-1} & |\Delta g|_{\max} &= 0.023 \text{ kJ kg}^{-1} \\ |\Delta c_p|_{\max} &= 0.78 \% & |\Delta w|_{\max} &= 0.051 \% . \end{aligned}$$

These maximum inconsistencies are clearly smaller than the consistency requirements on region boundaries corresponding to the so-called Prague values [13], which are given in Section 10.

Along the 10 MPa isobar in the metastable-vapor region, the transition between Eq. (18) and Eq. (15) is not smooth, which is however, not of importance for practical calculations.

Computer-program verification

To assist the user in computer-program verification of Eq. (18), Table 18 contains test values of the most relevant properties.

Table 18. Thermodynamic property values calculated from Eq. (18) for selected values of T and p ^a

	$T = 450 \text{ K},$ $p = 1 \text{ MPa}$	$T = 440 \text{ K},$ $p = 1 \text{ MPa}$	$T = 450 \text{ K},$ $p = 1.5 \text{ MPa}$
$v/(\text{m}^3 \text{ kg}^{-1})$	0.192 516 540	0.186 212 297	0.121 685 206
$h/(\text{kJ kg}^{-1})$	$0.276\ 881\ 115 \times 10^4$	$0.274\ 015\ 123 \times 10^4$	$0.272\ 134\ 539 \times 10^4$
$u/(\text{kJ kg}^{-1})$	$0.257\ 629\ 461 \times 10^4$	$0.255\ 393\ 894 \times 10^4$	$0.253\ 881\ 758 \times 10^4$
$s/(\text{kJ kg}^{-1} \text{ K}^{-1})$	$0.656\ 660\ 377 \times 10^1$	$0.650\ 218\ 759 \times 10^1$	$0.629\ 170\ 440 \times 10^1$
$c_p/(\text{kJ kg}^{-1} \text{ K}^{-1})$	$0.276\ 349\ 265 \times 10^1$	$0.298\ 166\ 443 \times 10^1$	$0.362\ 795\ 578 \times 10^1$
$w/(\text{m s}^{-1})$	$0.498\ 408\ 101 \times 10^3$	$0.489\ 363\ 295 \times 10^3$	$0.481\ 941\ 819 \times 10^3$

^a It is recommended to verify programmed functions using 8 byte real values for all three combinations of T and p given in this table.

6.3 Backward Equations

For the calculation of properties as function of p, h or of p, s without any iteration, the two backward equations require extremely good numerical consistency with the basic equation. The exact requirements for these numerical consistencies were obtained from comprehensive test calculations for several characteristic power cycles. The result of these investigations, namely the assignment of the tolerable numerical inconsistencies between the basic equation, Eq. (15), and the corresponding backward equations, is given in Tables 23 and 29, respectively.

Region 2 is covered by *three* $T(p, h)$ and *three* $T(p, s)$ equations. Figure 2 shows the way in which region 2 is divided into three subregions for the backward equations. The boundary between the subregions 2a and 2b is the isobar $p = 4 \text{ MPa}$; the boundary between the subregions 2b and 2c corresponds to the entropy line $s = 5.85 \text{ kJ kg}^{-1} \text{ K}^{-1}$.

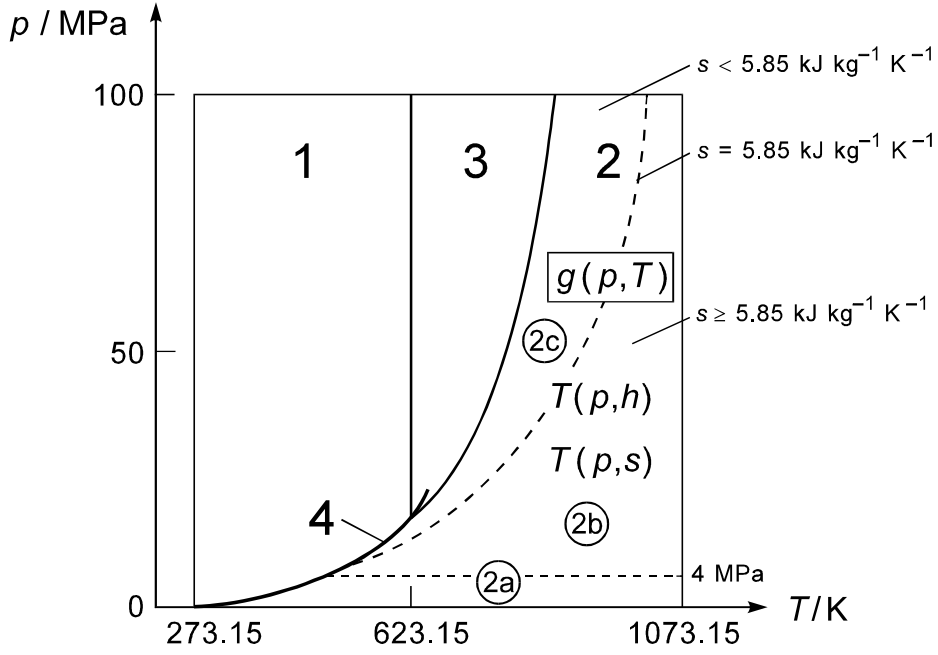


Fig. 2. Division of region 2 of IAPWS-IF97 into the three subregions 2a, 2b, and 2c for the backward equations $T(p, h)$ and $T(p, s)$.

In order to know whether the $T(p, h)$ equation for subregion 2b or for subregion 2c has to be used for given values of p and h , a special correlation equation for the boundary between subregions 2b and 2c (which approximates $s = 5.85 \text{ kJ kg}^{-1} \text{ K}^{-1}$) is needed; see Fig. 2. This boundary equation, called the B2bc-equation, is a simple quadratic pressure-enthalpy relation which reads

$$\pi = n_1 + n_2\eta + n_3\eta^2, \quad (20)$$

where $\pi = p/p^*$ and $\eta = h/h^*$ with $p^* = 1 \text{ MPa}$ and $h^* = 1 \text{ kJ kg}^{-1}$. The coefficients n_1 to n_3 of Eq. (20) are listed in Table 19. Based on its simple form, Eq. (20) does not describe exactly the isentropic line $s = 5.85 \text{ kJ kg}^{-1} \text{ K}^{-1}$; the entropy values corresponding to this p - h relation are between $s = 5.81 \text{ kJ kg}^{-1} \text{ K}^{-1}$ and $s = 5.85 \text{ kJ kg}^{-1} \text{ K}^{-1}$. The enthalpy-explicit form of Eq. (20) is as follows:

$$\eta = n_4 + [(\pi - n_5) / n_3]^{1/2}, \quad (21)$$

with π and η according to Eq. (20) and the coefficients n_3 to n_5 listed in Table 19. Equations (20) and (21) give the boundary line between subregions 2b and 2c from the saturation state at $T = 554.485 \text{ K}$ and $p_s = 6.54670 \text{ MPa}$ to $T = 1019.32 \text{ K}$ and $p = 100 \text{ MPa}$.

For the backward equations $T(p, s)$ the boundary between subregions 2b and 2c is, based on the value $s = 5.85 \text{ kJ kg}^{-1} \text{ K}^{-1}$ along this boundary, automatically defined for given values of p and s .

Table 19. Numerical values of the coefficients of the B2bc-equation, Eqs. (20) and (21), for defining the boundary between subregions 2b and 2c with respect to $T(p, h)$ calculations

i	n_i	i	n_i
1	$0.905\ 842\ 785\ 147\ 23 \times 10^3$	4	$0.265\ 265\ 719\ 084\ 28 \times 10^4$
2	$-0.679\ 557\ 863\ 992\ 41$	5	$0.452\ 575\ 789\ 059\ 48 \times 10^1$
3	$0.128\ 090\ 027\ 301\ 36 \times 10^{-3}$		

For *computer-program verification*, Eqs. (20) and (21) must meet the following p - h point: $p = 0.100\ 000\ 000 \times 10^3$ MPa , $h = 0.351\ 600\ 432\ 3 \times 10^4$ kJ kg⁻¹.

6.3.1 The Backward Equations $T(p, h)$ for Subregions 2a, 2b, and 2c

The backward equation $T(p, h)$ for **subregion 2a** in its dimensionless form reads

$$\frac{T_{2a}(p, h)}{T^*} = \theta_{2a}(\pi, \eta) = \sum_{i=1}^{34} n_i \pi^{I_i} (\eta - 2.1)^{J_i} , \quad (22)$$

where $\theta = T/T^*$, $\pi = p/p^*$, and $\eta = h/h^*$ with $T^* = 1$ K , $p^* = 1$ MPa, and $h^* = 2000$ kJ kg⁻¹. The coefficients n_i and exponents I_i and J_i of Eq. (22) are listed in Table 20.

Table 20. Numerical values of the coefficients and exponents of the backward equation $T(p, h)$ for subregion 2a, Eq. (22)

i	I_i	J_i	n_i	i	I_i	J_i	n_i
1	0	0	$0.108\ 989\ 523\ 182\ 88 \times 10^4$	18	2	7	$0.116\ 708\ 730\ 771\ 07 \times 10^2$
2	0	1	$0.849\ 516\ 544\ 955\ 35 \times 10^3$	19	2	36	$0.128\ 127\ 984\ 040\ 46 \times 10^9$
3	0	2	$-0.107\ 817\ 480\ 918\ 26 \times 10^3$	20	2	38	$-0.985\ 549\ 096\ 232\ 76 \times 10^9$
4	0	3	$0.331\ 536\ 548\ 012\ 63 \times 10^2$	21	2	40	$0.282\ 245\ 469\ 730\ 02 \times 10^{10}$
5	0	7	$-0.742\ 320\ 167\ 902\ 48 \times 10^1$	22	2	42	$-0.359\ 489\ 714\ 107\ 03 \times 10^{10}$
6	0	20	$0.117\ 650\ 487\ 243\ 56 \times 10^2$	23	2	44	$0.172\ 273\ 499\ 131\ 97 \times 10^{10}$
7	1	0	$0.184\ 457\ 493\ 557\ 90 \times 10^1$	24	3	24	$-0.135\ 513\ 342\ 407\ 75 \times 10^5$
8	1	1	$-0.417\ 927\ 005\ 496\ 24 \times 10^1$	25	3	44	$0.128\ 487\ 346\ 646\ 50 \times 10^8$
9	1	2	$0.624\ 781\ 969\ 358\ 12 \times 10^1$	26	4	12	$0.138\ 657\ 242\ 832\ 26 \times 10^1$
10	1	3	$-0.173\ 445\ 631\ 081\ 14 \times 10^2$	27	4	32	$0.235\ 988\ 325\ 565\ 14 \times 10^6$
11	1	7	$-0.200\ 581\ 768\ 620\ 96 \times 10^3$	28	4	44	$-0.131\ 052\ 365\ 450\ 54 \times 10^8$
12	1	9	$0.271\ 960\ 654\ 737\ 96 \times 10^3$	29	5	32	$0.739\ 998\ 354\ 747\ 66 \times 10^4$
13	1	11	$-0.455\ 113\ 182\ 858\ 18 \times 10^3$	30	5	36	$-0.551\ 966\ 970\ 300\ 60 \times 10^6$
14	1	18	$0.309\ 196\ 886\ 047\ 55 \times 10^4$	31	5	42	$0.371\ 540\ 859\ 962\ 33 \times 10^7$
15	1	44	$0.252\ 266\ 403\ 578\ 72 \times 10^6$	32	6	34	$0.191\ 277\ 292\ 396\ 60 \times 10^5$
16	2	0	$-0.617\ 074\ 228\ 683\ 39 \times 10^{-2}$	33	6	44	$-0.415\ 351\ 648\ 356\ 34 \times 10^6$
17	2	2	$-0.310\ 780\ 466\ 295\ 83$	34	7	28	$-0.624\ 598\ 551\ 925\ 07 \times 10^2$

The backward equation $T(p, h)$ for **subregion 2b** in its dimensionless form reads

$$\frac{T_{2b}(p, h)}{T^*} = \theta_{2b}(\pi, \eta) = \sum_{i=1}^{38} n_i (\pi - 2)^{I_i} (\eta - 2.6)^{J_i} , \quad (23)$$

where $\theta = T/T^*$, $\pi = p/p^*$, and $\eta = h/h^*$ with $T^* = 1$ K, $p^* = 1$ MPa, and $h^* = 2000$ kJ kg⁻¹. The coefficients n_i and exponents I_i and J_i of Eq. (23) are listed in Table 21.

Table 21. Numerical values of the coefficients and exponents of the backward equation $T(p, h)$ for subregion 2b, Eq. (23)

i	I_i	J_i	n_i	i	I_i	J_i	n_i
1	0	0	0.148 950 410 795 16 × 10 ⁴	20	2	40	0.712 803 519 595 51 × 10 ⁻⁴
2	0	1	0.743 077 983 140 34 × 10 ³	21	3	1	0.110 328 317 899 99 × 10 ⁻³
3	0	2	-0.977 083 187 978 37 × 10 ²	22	3	2	0.189 552 483 879 02 × 10 ⁻³
4	0	12	0.247 424 647 056 74 × 10 ¹	23	3	12	0.308 915 411 605 37 × 10 ⁻²
5	0	18	-0.632 813 200 160 26	24	3	24	0.135 555 045 549 49 × 10 ⁻²
6	0	24	0.113 859 521 296 58 × 10 ¹	25	4	2	0.286 402 374 774 56 × 10 ⁻⁶
7	0	28	-0.478 118 636 486 25	26	4	12	-0.107 798 573 575 12 × 10 ⁻⁴
8	0	40	0.852 081 234 315 44 × 10 ⁻²	27	4	18	-0.764 627 124 548 14 × 10 ⁻⁴
9	1	0	0.937 471 473 779 32	28	4	24	0.140 523 928 183 16 × 10 ⁻⁴
10	1	2	0.335 931 186 049 16 × 10 ¹	29	4	28	-0.310 838 143 314 34 × 10 ⁻⁴
11	1	6	0.338 093 556 014 54 × 10 ¹	30	4	40	-0.103 027 382 121 03 × 10 ⁻⁵
12	1	12	0.168 445 396 719 04	31	5	18	0.282 172 816 350 40 × 10 ⁻⁶
13	1	18	0.738 757 452 366 95	32	5	24	0.127 049 022 719 45 × 10 ⁻⁵
14	1	24	-0.471 287 374 361 86	33	5	40	0.738 033 534 682 92 × 10 ⁻⁷
15	1	28	0.150 202 731 397 07	34	6	28	-0.110 301 392 389 09 × 10 ⁻⁷
16	1	40	-0.217 641 142 197 50 × 10 ⁻²	35	7	2	-0.814 563 652 078 33 × 10 ⁻¹³
17	2	2	-0.218 107 553 247 61 × 10 ⁻¹	36	7	28	-0.251 805 456 829 62 × 10 ⁻¹⁰
18	2	8	-0.108 297 844 036 77	37	9	1	-0.175 652 339 694 07 × 10 ⁻¹⁷
19	2	18	-0.463 333 246 358 12 × 10 ⁻¹	38	9	40	0.869 341 563 441 63 × 10 ⁻¹⁴

The backward equation $T(p,h)$ for **subregion 2c** in its dimensionless form reads

$$\frac{T_{2c}(p,h)}{T^*} = \theta_{2c}(\pi,\eta) = \sum_{i=1}^{23} n_i (\pi + 25)^{I_i} (\eta - 1.8)^{J_i}, \quad (24)$$

where $\theta = T/T^*$, $\pi = p/p^*$, and $\eta = h/h^*$ with $T^* = 1$ K, $p^* = 1$ MPa, and $h^* = 2000$ kJ kg⁻¹. The coefficients n_i and exponents I_i and J_i of Eq. (24) are listed in Table 22.

Table 22. Numerical values of the coefficients and exponents of the backward equation $T(p,h)$ for subregion 2c, Eq. (24)

i	I_i	J_i	n_i
1	-7	0	$-0.323\ 683\ 985\ 552\ 42 \times 10^{13}$
2	-7	4	$0.732\ 633\ 509\ 021\ 81 \times 10^{13}$
3	-6	0	$0.358\ 250\ 899\ 454\ 47 \times 10^{12}$
4	-6	2	$-0.583\ 401\ 318\ 515\ 90 \times 10^{12}$
5	-5	0	$-0.107\ 830\ 682\ 174\ 70 \times 10^{11}$
6	-5	2	$0.208\ 255\ 445\ 631\ 71 \times 10^{11}$
7	-2	0	$0.610\ 747\ 835\ 645\ 16 \times 10^6$
8	-2	1	$0.859\ 777\ 225\ 355\ 80 \times 10^6$
9	-1	0	$-0.257\ 457\ 236\ 041\ 70 \times 10^5$
10	-1	2	$0.310\ 810\ 884\ 227\ 14 \times 10^5$
11	0	0	$0.120\ 823\ 158\ 659\ 36 \times 10^4$
12	0	1	$0.482\ 197\ 551\ 092\ 55 \times 10^3$
13	1	4	$0.379\ 660\ 012\ 724\ 86 \times 10^1$
14	1	8	$-0.108\ 429\ 848\ 800\ 77 \times 10^2$
15	2	4	$-0.453\ 641\ 726\ 766\ 60 \times 10^{-1}$
16	6	0	$0.145\ 591\ 156\ 586\ 98 \times 10^{-12}$
17	6	1	$0.112\ 615\ 974\ 072\ 30 \times 10^{-11}$
18	6	4	$-0.178\ 049\ 822\ 406\ 86 \times 10^{-10}$
19	6	10	$0.123\ 245\ 796\ 908\ 32 \times 10^{-6}$
20	6	12	$-0.116\ 069\ 211\ 309\ 84 \times 10^{-5}$
21	6	16	$0.278\ 463\ 670\ 885\ 54 \times 10^{-4}$
22	6	20	$-0.592\ 700\ 384\ 741\ 76 \times 10^{-3}$
23	6	22	$0.129\ 185\ 829\ 918\ 78 \times 10^{-2}$

Range of validity

Equations (22), (23), and (24) are only valid in the respective subregion 2a, 2b, and 2c which do not include the metastable-vapor region. The boundaries between these subregions are defined at the beginning of Section 6.3; the lowest pressure for which Eq. (22) is valid amounts to 611.153 Pa corresponding to the sublimation pressure [10] at 273.15 K.

Numerical consistency with the basic equation

For ten million random pairs of p and h covering each of the subregions 2a, 2b, and 2c, the differences ΔT between temperatures calculated from Eqs. (22) to (24), respectively, and from Eq. (15) were determined. The corresponding maximum and root-mean-square differences are listed in Table 23 together with the tolerated differences according to the numerical consistency requirements with respect to Eq. (15).

Table 23. Maximum differences $|\Delta T|_{\max}$ and root-mean-square differences ΔT_{RMS} between temperatures calculated from Eqs. (22) to (24), and from Eq. (15) in comparison with the tolerated differences $|\Delta T|_{\text{tol}}$

Subregion	Equation	$ \Delta T _{\text{tol}}/\text{mK}$	$ \Delta T _{\max}/\text{mK}$	$\Delta T_{\text{RMS}}/\text{mK}$
2a	22	10	9.3	2.9
2b	23	10	9.6	3.9
2c	24	25	23.7	10.4

Computer-program verification

To assist the user in computer-program verification of Eqs. (22) to (24), Table 24 contains the corresponding test values.

Table 24. Temperature values calculated from Eqs. (22) to (24) for selected values of p and h ^a

Equation	p/MPa	$h/(\text{kJ kg}^{-1})$	T/K
22	0.001	3000	$0.534\ 433\ 241 \times 10^3$
	3	3000	$0.575\ 373\ 370 \times 10^3$
	3	4000	$0.101\ 077\ 577 \times 10^4$
23	5	3500	$0.801\ 299\ 102 \times 10^3$
	5	4000	$0.101\ 531\ 583 \times 10^4$
	25	3500	$0.875\ 279\ 054 \times 10^3$
24	40	2700	$0.743\ 056\ 411 \times 10^3$
	60	2700	$0.791\ 137\ 067 \times 10^3$
	60	3200	$0.882\ 756\ 860 \times 10^3$

^a It is recommended to verify the programmed equations using 8 byte real values for all three combinations of p and h given in this table for each of the equations.

6.3.2 The Backward Equations $T(p, s)$ for Subregions 2a, 2b, and 2c

The backward equation $T(p, s)$ for **subregion 2a** in its dimensionless form reads

$$\frac{T_{2a}(p, s)}{T^*} = \theta_{2a}(\pi, \sigma) = \sum_{i=1}^{46} n_i \pi^{I_i} (\sigma - 2)^{J_i}, \quad (25)$$

where $\theta = T/T^*$, $\pi = p/p^*$, and $\sigma = s/s^*$ with $T^* = 1$ K, $p^* = 1$ MPa, and $s^* = 2$ kJ kg⁻¹ K⁻¹. The coefficients n_i and exponents I_i and J_i of Eq. (25) are listed in Table 25.

Table 25. Numerical values of the coefficients and exponents of the backward equation $T(p, s)$ for subregion 2a, Eq. (25)

i	I_i	J_i	n_i	i	I_i	J_i	n_i
1	-1.5	-24	-0.392 359 838 619 84 × 10 ⁶	24	-0.25	-11	-0.597 806 388 727 18 × 10 ⁴
2	-1.5	-23	0.515 265 738 272 70 × 10 ⁶	25	-0.25	-6	-0.704 014 639 268 62 × 10 ³
3	-1.5	-19	0.404 824 431 610 48 × 10 ⁵	26	0.25	1	0.338 367 841 075 53 × 10 ³
4	-1.5	-13	-0.321 937 909 239 02 × 10 ³	27	0.25	4	0.208 627 866 351 87 × 10 ²
5	-1.5	-11	0.969 614 242 186 94 × 10 ²	28	0.25	8	0.338 341 726 561 96 × 10 ⁻¹
6	-1.5	-10	-0.228 678 463 717 73 × 10 ²	29	0.25	11	-0.431 244 284 148 93 × 10 ⁻⁴
7	-1.25	-19	-0.449 429 141 243 57 × 10 ⁶	30	0.50	0	0.166 537 913 564 12 × 10 ³
8	-1.25	-15	-0.501 183 360 201 66 × 10 ⁴	31	0.5	1	-0.139 862 920 558 98 × 10 ³
9	-1.25	-6	0.356 844 635 600 15	32	0.5	5	-0.788 495 479 998 72
10	-1.0	-26	0.442 353 358 481 90 × 10 ⁵	33	0.5	6	0.721 324 117 538 72 × 10 ⁻¹
11	-1.0	-21	-0.136 733 888 117 08 × 10 ⁵	34	0.5	10	-0.597 548 393 982 83 × 10 ⁻²
12	-1.0	-17	0.421 632 602 078 64 × 10 ⁶	35	0.5	14	-0.121 413 589 539 04 × 10 ⁻⁴
13	-1.0	-16	0.225 169 258 374 75 × 10 ⁵	36	0.5	16	0.232 270 967 338 71 × 10 ⁻⁶
14	-1.0	-9	0.474 421 448 656 46 × 10 ³	37	0.75	0	-0.105 384 635 661 94 × 10 ²
15	-1.0	-8	-0.149 311 307 976 47 × 10 ³	38	0.75	4	0.207 189 254 965 02 × 10 ¹
16	-0.75	-15	-0.197 811 263 204 52 × 10 ⁶	39	0.75	9	-0.721 931 552 604 27 × 10 ⁻¹
17	-0.75	-14	-0.235 543 994 707 60 × 10 ⁵	40	0.75	17	0.207 498 870 811 20 × 10 ⁻⁶
18	-0.5	-26	-0.190 706 163 020 76 × 10 ⁵	41	1.0	7	-0.183 406 579 113 79 × 10 ⁻¹
19	-0.5	-13	0.553 756 698 831 64 × 10 ⁵	42	1.0	18	0.290 362 723 486 96 × 10 ⁻⁶
20	-0.5	-9	0.382 936 914 373 63 × 10 ⁴	43	1.25	3	0.210 375 278 936 19
21	-0.5	-7	-0.603 918 605 805 67 × 10 ³	44	1.25	15	0.256 812 397 299 99 × 10 ⁻³
22	-0.25	-27	0.193 631 026 203 31 × 10 ⁴	45	1.5	5	-0.127 990 029 337 81 × 10 ⁻¹
23	-0.25	-25	0.426 606 436 986 10 × 10 ⁴	46	1.5	18	-0.821 981 026 520 18 × 10 ⁻⁵

The backward equation $T(p, s)$ for **subregion 2b** in its dimensionless form reads

$$\frac{T_{2b}(p, s)}{T^*} = \theta_{2b}(\pi, \sigma) = \sum_{i=1}^{44} n_i \pi^{I_i} (10 - \sigma)^{J_i}, \quad (26)$$

where $\theta = T/T^*$, $\pi = p/p^*$, and $\sigma = s/s^*$ with $T^* = 1 \text{ K}$, $p^* = 1 \text{ MPa}$, and $s^* = 0.7853 \text{ kJ kg}^{-1} \text{ K}^{-1}$. The coefficients n_i and exponents I_i and J_i of Eq. (26) are listed in Table 26.

Table 26. Numerical values of the coefficients and exponents of the backward equation $T(p, s)$ for subregion 2b, Eq. (26)

i	I_i	J_i	n_i	i	I_i	J_i	n_i
1	-6	0	0.316 876 650 834 97 $\times 10^6$	23	0	2	0.417 273 471 596 10 $\times 10^2$
2	-6	11	0.208 641 758 818 58 $\times 10^2$	24	0	4	0.219 325 494 345 32 $\times 10^1$
3	-5	0	-0.398 593 998 035 99 $\times 10^6$	25	0	5	-0.103 200 500 090 77 $\times 10^1$
4	-5	11	-0.218 160 585 188 77 $\times 10^2$	26	0	6	0.358 829 435 167 03
5	-4	0	0.223 697 851 942 42 $\times 10^6$	27	0	9	0.525 114 537 260 66 $\times 10^{-2}$
6	-4	1	-0.278 417 034 458 17 $\times 10^4$	28	1	0	0.128 389 164 507 05 $\times 10^2$
7	-4	11	0.992 074 360 714 80 $\times 10^1$	29	1	1	-0.286 424 372 193 81 $\times 10^1$
8	-3	0	-0.751 975 122 991 57 $\times 10^5$	30	1	2	0.569 126 836 648 55
9	-3	1	0.297 086 059 511 58 $\times 10^4$	31	1	3	-0.999 629 545 849 31 $\times 10^{-1}$
10	-3	11	-0.344 068 785 485 26 $\times 10^1$	32	1	7	-0.326 320 377 784 59 $\times 10^{-2}$
11	-3	12	0.388 155 642 491 15	33	1	8	0.233 209 225 767 23 $\times 10^{-3}$
12	-2	0	0.175 112 950 857 50 $\times 10^5$	34	2	0	-0.153 348 098 574 50
13	-2	1	-0.142 371 128 544 49 $\times 10^4$	35	2	1	0.290 722 882 399 02 $\times 10^{-1}$
14	-2	6	0.109 438 033 641 67 $\times 10^1$	36	2	5	0.375 347 027 411 67 $\times 10^{-3}$
15	-2	10	0.899 716 193 084 95	37	3	0	0.172 966 917 024 11 $\times 10^{-2}$
16	-1	0	-0.337 597 400 989 58 $\times 10^4$	38	3	1	-0.385 560 508 445 04 $\times 10^{-3}$
17	-1	1	0.471 628 858 183 55 $\times 10^3$	39	3	3	-0.350 177 122 926 08 $\times 10^{-4}$
18	-1	5	-0.191 882 419 936 79 $\times 10^1$	40	4	0	-0.145 663 936 314 92 $\times 10^{-4}$
19	-1	8	0.410 785 804 921 96	41	4	1	0.564 208 572 672 69 $\times 10^{-5}$
20	-1	9	-0.334 653 781 720 97	42	5	0	0.412 861 500 746 05 $\times 10^{-7}$
21	0	0	0.138 700 347 775 05 $\times 10^4$	43	5	1	-0.206 846 711 188 24 $\times 10^{-7}$
22	0	1	-0.406 633 261 958 38 $\times 10^3$	44	5	2	0.164 093 936 747 25 $\times 10^{-8}$

The backward equation $T(p, s)$ for **subregion 2c** in its dimensionless form reads

$$\frac{T_{2c}(p, s)}{T^*} = \theta_{2c}(\pi, \sigma) = \sum_{i=1}^{30} n_i \pi^{I_i} (2 - \sigma)^{J_i}, \quad (27)$$

where $\theta = T/T^*$, $\pi = p/p^*$, and $\sigma = s/s^*$ with $T^* = 1 \text{ K}$, $p^* = 1 \text{ MPa}$, and $s^* = 2.9251 \text{ kJ kg}^{-1} \text{ K}^{-1}$. The coefficients n_i and exponents I_i and J_i of Eq. (27) are listed in Table 27.

Table 27. Numerical values of the coefficients and exponents of the backward equation $T(p, s)$ for subregion 2c, Eq. (27)

i	I_i	J_i	n_i	i	I_i	J_i	n_i
1	-2	0	0.909 685 010 053 65 $\times 10^3$	16	3	1	-0.145 970 082 847 53 $\times 10^{-1}$
2	-2	1	0.240 456 670 884 20 $\times 10^4$	17	3	5	0.566 311 756 310 27 $\times 10^{-2}$
3	-1	0	-0.591 623 263 871 30 $\times 10^3$	18	4	0	-0.761 558 645 845 77 $\times 10^{-4}$
4	0	0	0.541 454 041 280 74 $\times 10^3$	19	4	1	0.224 403 429 193 32 $\times 10^{-3}$
5	0	1	-0.270 983 084 111 92 $\times 10^3$	20	4	4	-0.125 610 950 134 13 $\times 10^{-4}$
6	0	2	0.979 765 250 979 26 $\times 10^3$	21	5	0	0.633 231 326 609 34 $\times 10^{-6}$
7	0	3	-0.469 667 729 594 35 $\times 10^3$	22	5	1	-0.205 419 896 753 75 $\times 10^{-5}$
8	1	0	0.143 992 746 047 23 $\times 10^2$	23	5	2	0.364 053 703 900 82 $\times 10^{-7}$
9	1	1	-0.191 042 042 304 29 $\times 10^2$	24	6	0	-0.297 598 977 892 15 $\times 10^{-8}$
10	1	3	0.532 991 671 119 71 $\times 10^1$	25	6	1	0.101 366 185 297 63 $\times 10^{-7}$
11	1	4	-0.212 529 753 759 34 $\times 10^2$	26	7	0	0.599 257 196 923 51 $\times 10^{-11}$
12	2	0	-0.311 473 344 137 60	27	7	1	-0.206 778 701 051 64 $\times 10^{-10}$
13	2	1	0.603 348 408 946 23	28	7	3	-0.208 742 781 818 86 $\times 10^{-10}$
14	2	2	-0.427 648 397 025 09 $\times 10^{-1}$	29	7	4	0.101 621 668 250 89 $\times 10^{-9}$
15	3	0	0.581 855 972 552 59 $\times 10^{-2}$	30	7	5	-0.164 298 282 813 47 $\times 10^{-9}$

Range of validity

Equations (25), (26), and (27) are only valid in the respective subregion 2a, 2b, and 2c which do not include the metastable-vapor region. The boundaries between these subregions are defined at the beginning of Section 6.3; the lowest pressure for which Eq. (25) is valid amounts to 611.153 Pa corresponding to the sublimation pressure [10] at 273.15 K.

Numerical consistency with the basic equation

For ten million random pairs of p and s covering each of the subregions 2a, 2b, and 2c, the differences ΔT between temperatures calculated from Eqs. (25) to (27), respectively, and from Eq. (15) were determined. The corresponding maximum and root-mean-square differences are listed in Table 28 together with the tolerated differences according to the numerical consistency requirements with respect to Eq. (15).

Table 28. Maximum differences $|\Delta T|_{\max}$ and root-mean-square differences ΔT_{RMS} between temperatures calculated from Eqs. (25) to (27), and from Eq. (15) in comparison with the tolerated differences $|\Delta T|_{\text{tol}}$

Subregion	Equation	$ \Delta T _{\text{tol}}/\text{mK}$	$ \Delta T _{\max}/\text{mK}$	$\Delta T_{\text{RMS}}/\text{mK}$
2a	25	10	8.8	1.2
2b	26	10	6.5	2.8
2c	27	25	19.0	8.3

Computer-program verification

To assist the user in computer-program verification of Eqs. (25) to (27), Table 29 contains the corresponding test values.

Table 29. Temperature values calculated from Eqs. (25) to (27) for selected values of p and s ^a

Equation	p/MPa	$s/(\text{kJ kg}^{-1} \text{K}^{-1})$	T/K
25	0.1	7.5	$0.399\ 517\ 097 \times 10^3$
	0.1	8	$0.514\ 127\ 081 \times 10^3$
	2.5	8	$0.103\ 984\ 917 \times 10^4$
26	8	6	$0.600\ 484\ 040 \times 10^3$
	8	7.5	$0.106\ 495\ 556 \times 10^4$
	90	6	$0.103\ 801\ 126 \times 10^4$
27	20	5.75	$0.697\ 992\ 849 \times 10^3$
	80	5.25	$0.854\ 011\ 484 \times 10^3$
	80	5.75	$0.949\ 017\ 998 \times 10^3$

^a It is recommended to verify the programmed equations using 8 byte real values for all three combinations of p and s given in this table for each of the equations.

7 Basic Equation for Region 3

This section contains all details relevant for the use of the basic equation of region 3 of IAPWS-IF97. Information about the consistency of the basic equation of this region with the basic equations of regions 1, 2, and 4 along the corresponding region boundaries is summarized in Section 10. The auxiliary equation for defining the boundary between regions 2 and 3 is given in Section 4. Section 11 contains the results of computing-time comparisons between IAPWS-IF97 and IFC-67. The estimates of uncertainty of the most relevant properties can be found in Section 12.

The basic equation for this region is a fundamental equation for the specific Helmholtz free energy f . This equation is expressed in dimensionless form, $\phi = f/(RT)$, and reads

$$\frac{f(\rho, T)}{RT} = \phi(\delta, \tau) = n_1 \ln \delta + \sum_{i=2}^{40} n_i \delta^{I_i} \tau^{J_i}, \quad (28)$$

where $\delta = \rho/\rho^*$, $\tau = T^*/T$ with $\rho^* = \rho_c$, $T^* = T_c$ and R , T_c , and ρ_c given by Eqs. (1), (2), and (4). The coefficients n_i and exponents I_i and J_i of Eq. (28) are listed in Table 30.

In addition to representing the thermodynamic properties in the single-phase region, Eq. (28) meets the phase-equilibrium condition (equality of specific Gibbs free energy for coexisting vapor + liquid states; see Table 31) along the saturation line for $T \geq 623.15$ K to T_c . Moreover, Eq. (28) reproduces exactly the critical parameters according to Eqs. (2) to (4) and yields zero for the first two pressure derivatives with respect to density at the critical point.

Table 30. Numerical values of the coefficients and exponents of the dimensionless Helmholtz free energy for region 3, Eq. (28)

i	I_i	J_i	n_i	i	I_i	J_i	n_i
1	0	0	$0.106\ 580\ 700\ 285\ 13 \times 10^1$	21	3	4	$-0.201\ 899\ 150\ 235\ 70 \times 10^1$
2	0	0	$-0.157\ 328\ 452\ 902\ 39 \times 10^2$	22	3	16	$-0.821\ 476\ 371\ 739\ 63 \times 10^{-2}$
3	0	1	$0.209\ 443\ 969\ 743\ 07 \times 10^2$	23	3	26	$-0.475\ 960\ 357\ 349\ 23$
4	0	2	$-0.768\ 677\ 078\ 787\ 16 \times 10^1$	24	4	0	$0.439\ 840\ 744\ 735\ 00 \times 10^{-1}$
5	0	7	$0.261\ 859\ 477\ 879\ 54 \times 10^1$	25	4	2	$-0.444\ 764\ 354\ 287\ 39$
6	0	10	$-0.280\ 807\ 811\ 486\ 20 \times 10^1$	26	4	4	$0.905\ 720\ 707\ 197\ 33$
7	0	12	$0.120\ 533\ 696\ 965\ 17 \times 10^1$	27	4	26	$0.705\ 224\ 500\ 879\ 67$
8	0	23	$-0.845\ 668\ 128\ 125\ 02 \times 10^{-2}$	28	5	1	$0.107\ 705\ 126\ 263\ 32$
9	1	2	$-0.126\ 543\ 154\ 777\ 14 \times 10^1$	29	5	3	$-0.329\ 136\ 232\ 589\ 54$
10	1	6	$-0.115\ 244\ 078\ 066\ 81 \times 10^1$	30	5	26	$-0.508\ 710\ 620\ 411\ 58$
11	1	15	$0.885\ 210\ 439\ 843\ 18$	31	6	0	$-0.221\ 754\ 008\ 730\ 96 \times 10^{-1}$
12	1	17	$-0.642\ 077\ 651\ 816\ 07$	32	6	2	$0.942\ 607\ 516\ 650\ 92 \times 10^{-1}$
13	2	0	$0.384\ 934\ 601\ 866\ 71$	33	6	26	$0.164\ 362\ 784\ 479\ 61$
14	2	2	$-0.852\ 147\ 088\ 242\ 06$	34	7	2	$-0.135\ 033\ 722\ 413\ 48 \times 10^{-1}$
15	2	6	$0.489\ 722\ 815\ 418\ 77 \times 10^1$	35	8	26	$-0.148\ 343\ 453\ 524\ 72 \times 10^{-1}$
16	2	7	$-0.305\ 026\ 172\ 569\ 65 \times 10^1$	36	9	2	$0.579\ 229\ 536\ 280\ 84 \times 10^{-3}$
17	2	22	$0.394\ 205\ 368\ 791\ 54 \times 10^{-1}$	37	9	26	$0.323\ 089\ 047\ 037\ 11 \times 10^{-2}$
18	2	26	$0.125\ 584\ 084\ 243\ 08$	38	10	0	$0.809\ 648\ 029\ 962\ 15 \times 10^{-4}$
19	3	0	$-0.279\ 993\ 296\ 987\ 10$	39	10	1	$-0.165\ 576\ 797\ 950\ 37 \times 10^{-3}$
20	3	2	$0.138\ 997\ 995\ 694\ 60 \times 10^1$	40	11	26	$-0.449\ 238\ 990\ 618\ 15 \times 10^{-4}$

All thermodynamic properties can be derived from Eq. (28) by using the appropriate combinations of the dimensionless Helmholtz free energy and its derivatives. Relations between the relevant thermodynamic properties and ϕ and its derivatives are summarized in Table 31. All required derivatives of the dimensionless Helmholtz free energy are explicitly given in Table 32.

Table 31. Relations of thermodynamic properties to the dimensionless Helmholtz free energy ϕ and its derivatives ^a when using Eq. (28)

Property	Relation
Pressure $p = \rho^2 (\partial f / \partial \rho)_T$	$\frac{p(\delta, \tau)}{\rho RT} = \delta \phi_\delta$
Specific internal energy $u = f - T(\partial f / \partial T)_\rho$	$\frac{u(\delta, \tau)}{RT} = \tau \phi_\tau$
Specific entropy $s = -(\partial f / \partial T)_\rho$	$\frac{s(\delta, \tau)}{R} = \tau \phi_\tau - \phi$
Specific enthalpy $h = f - T(\partial f / \partial T)_\rho + \rho(\partial f / \partial \rho)_T$	$\frac{h(\delta, \tau)}{RT} = \tau \phi_\tau + \delta \phi_\delta$
Specific isochoric heat capacity $c_v = (\partial u / \partial T)_\rho$	$\frac{c_v(\delta, \tau)}{R} = -\tau^2 \phi_{\tau\tau}$
Specific isobaric heat capacity $c_p = (\partial h / \partial T)_p$	$\frac{c_p(\delta, \tau)}{R} = -\tau^2 \phi_{\tau\tau} + \frac{(\delta \phi_\delta - \delta \tau \phi_{\delta\tau})^2}{2\delta \phi_\delta + \delta^2 \phi_{\delta\delta}}$
Speed of sound $w = (\partial p / \partial \rho)_s^{1/2}$	$\frac{w^2(\delta, \tau)}{RT} = 2\delta \phi_\delta + \delta^2 \phi_{\delta\delta} - \frac{(\delta \phi_\delta - \delta \tau \phi_{\delta\tau})^2}{\tau^2 \phi_{\tau\tau}}$
Phase-equilibrium condition (Maxwell criterion)	$\frac{p_s}{RT\rho'} = \delta' \phi_\delta(\delta', \tau) \quad ; \quad \frac{p_s}{RT\rho''} = \delta'' \phi_\delta(\delta'', \tau)$ $\frac{p_s}{RT} \left(\frac{1}{\rho''} - \frac{1}{\rho'} \right) = \phi(\delta', \tau) - \phi(\delta'', \tau)$

$$^a \quad \phi_\delta = \left[\frac{\partial \phi}{\partial \delta} \right]_\tau, \quad \phi_{\delta\delta} = \left[\frac{\partial^2 \phi}{\partial \delta^2} \right]_\tau, \quad \phi_\tau = \left[\frac{\partial \phi}{\partial \tau} \right]_\delta, \quad \phi_{\tau\tau} = \left[\frac{\partial^2 \phi}{\partial \tau^2} \right]_\delta, \quad \phi_{\delta\tau} = \left[\frac{\partial^2 \phi}{\partial \delta \partial \tau} \right]$$

Table 32. The dimensionless Helmholtz free energy equation and its derivatives ^a according to Eq. (28)

$$\phi = n_1 \ln \delta + \sum_{i=2}^{40} n_i \delta^{I_i} \tau^{J_i}$$

$$\phi_\delta = n_1 / \delta + \sum_{i=2}^{40} n_i I_i \delta^{I_i-1} \tau^{J_i} \quad \phi_{\delta\delta} = -n_1 / \delta^2 + \sum_{i=2}^{40} n_i I_i(I_i-1) \delta^{I_i-2} \tau^{J_i}$$

$$\phi_\tau = 0 + \sum_{i=2}^{40} n_i \delta^{I_i} J_i \tau^{J_i-1} \quad \phi_{\tau\tau} = 0 + \sum_{i=2}^{40} n_i \delta^{I_i} J_i(J_i-1) \tau^{J_i-2}$$

$$\phi_{\delta\tau} = 0 + \sum_{i=2}^{40} n_i I_i \delta^{I_i-1} J_i \tau^{J_i-1}$$

$$^a \quad \phi_\delta = \left[\frac{\partial \phi}{\partial \delta} \right]_\tau, \quad \phi_{\delta\delta} = \left[\frac{\partial^2 \phi}{\partial \delta^2} \right]_\tau, \quad \phi_\tau = \left[\frac{\partial \phi}{\partial \tau} \right]_\delta, \quad \phi_{\tau\tau} = \left[\frac{\partial^2 \phi}{\partial \tau^2} \right]_\delta, \quad \phi_{\delta\tau} = \left[\frac{\partial^2 \phi}{\partial \delta \partial \tau} \right]$$

Range of validity

Equation (28) covers region 3 of IAPWS-IF97 defined by the following range of temperature and pressure, see Fig. 1:

$$623.15 \text{ K} \leq T \leq T(p)_{\text{Eq.(6)}} \quad p(T)_{\text{Eq.(5)}} \leq p \leq 100 \text{ MPa} .$$

In addition to the properties in the stable single-phase region defined above, Eq.(28) also yields reasonable values in the metastable regions (superheated liquid and subcooled steam) close to the saturated liquid and saturated vapor line.

Computer-program verification

To assist the user in computer-program verification of Eq. (28), Table 33 contains test values of the most relevant properties.

Table 33. Thermodynamic property values calculated from Eq. (28), for selected values of T and ρ ^a

	$T = 650 \text{ K},$ $\rho = 500 \text{ kg m}^{-3}$	$T = 650 \text{ K},$ $\rho = 200 \text{ kg m}^{-3}$	$T = 750 \text{ K},$ $\rho = 500 \text{ kg m}^{-3}$
p/MPa	$0.255\ 837\ 018 \times 10^2$	$0.222\ 930\ 643 \times 10^2$	$0.783\ 095\ 639 \times 10^2$
$h/(\text{kJ kg}^{-1})$	$0.186\ 343\ 019 \times 10^4$	$0.237\ 512\ 401 \times 10^4$	$0.225\ 868\ 845 \times 10^4$
$u/(\text{kJ kg}^{-1})$	$0.181\ 226\ 279 \times 10^4$	$0.226\ 365\ 868 \times 10^4$	$0.210\ 206\ 932 \times 10^4$
$s/(\text{kJ kg}^{-1} \text{ K}^{-1})$	$0.405\ 427\ 273 \times 10^1$	$0.485\ 438\ 792 \times 10^1$	$0.446\ 971\ 906 \times 10^1$
$c_p/(\text{kJ kg}^{-1} \text{ K}^{-1})$	$0.138\ 935\ 717 \times 10^2$	$0.446\ 579\ 342 \times 10^2$	$0.634\ 165\ 359 \times 10^1$
$w/(\text{m s}^{-1})$	$0.502\ 005\ 554 \times 10^3$	$0.383\ 444\ 594 \times 10^3$	$0.760\ 696\ 041 \times 10^3$

^a It is recommended to verify programmed functions using 8 byte real values for all three combinations of T and ρ given in this table.

8 Equations for Region 4

This section contains all details relevant for the use of the equations for region 4 of IAPWS-IF97 (saturation line). Information about the consistency of the basic equation for this region, the saturation-pressure equation, and the basic equations of regions 1 to 3 at the corresponding region boundaries is summarized in Section 10. The results of computing-time comparisons between IAPWS-IF97 and IFC-67 are given in Section 11. The estimates of uncertainty of the saturation pressure can be found in Section 12.

The equation for describing the saturation line is an implicit quadratic equation which can be directly solved with regard to both saturation pressure p_s and saturation temperature T_s . This equation reads

$$\beta^2 \vartheta^2 + n_1 \beta^2 \vartheta + n_2 \beta^2 + n_3 \beta \vartheta^2 + n_4 \beta \vartheta + n_5 \beta + n_6 \vartheta^2 + n_7 \vartheta + n_8 = 0, \quad (29)$$

where
$$\beta = (p_s / p^*)^{1/4} \quad (29a)$$

and
$$\vartheta = \frac{T_s}{T^*} + \frac{n_9}{(T_s / T^*) - n_{10}} \quad (29b)$$

with $p^* = 1$ MPa and $T^* = 1$ K; for the coefficients n_1 to n_{10} see Table 34.

8.1 The Saturation-Pressure Equation (Basic Equation)

The solution of Eq. (29) with regard to saturation pressure is as follows:

$$\frac{p_s}{p^*} = \left[\frac{2C}{-B + (B^2 - 4AC)^{1/2}} \right]^4 \quad (30)$$

where $p^* = 1$ MPa and

$$A = \vartheta^2 + n_1\vartheta + n_2$$

$$B = n_3\vartheta^2 + n_4\vartheta + n_5$$

$$C = n_6\vartheta^2 + n_7\vartheta + n_8$$

with ϑ according to Eq. (29b). The coefficients n_i of Eq. (30) are listed in Table 34.

Table 34. Numerical values of the coefficients of the dimensionless saturation equations, Eqs. (29) to (31)

i	n_i	i	n_i
1	$0.116\ 705\ 214\ 527\ 67 \times 10^4$	6	$0.149\ 151\ 086\ 135\ 30 \times 10^2$
2	$-0.724\ 213\ 167\ 032\ 06 \times 10^6$	7	$-0.482\ 326\ 573\ 615\ 91 \times 10^4$
3	$-0.170\ 738\ 469\ 400\ 92 \times 10^2$	8	$0.405\ 113\ 405\ 420\ 57 \times 10^6$
4	$0.120\ 208\ 247\ 024\ 70 \times 10^5$	9	$-0.238\ 555\ 575\ 678\ 49$
5	$-0.323\ 255\ 503\ 223\ 33 \times 10^7$	10	$0.650\ 175\ 348\ 447\ 98 \times 10^3$

Equations (29) to (31) reproduce exactly the p - T values at the triple point according to Eq. (8), at the normal boiling point [12] and at the critical point according to Eqs. (2) and (3).

Range of validity

Equation (30) is valid along the entire vapor-liquid saturation line from the triple-point temperature T_t to the critical temperature T_c and can be simply extrapolated to 273.15 K so that it covers the temperature range

$$273.15 \text{ K} \leq T \leq 647.096 \text{ K} .$$

Computer-program verification

To assist the user in computer-program verification of Eq. (30), Table 35 contains test values for three selected temperatures.

Table 35. Saturation pressures calculated from Eq. (30) for selected values of T^a

T/K	p_s/MPa
300	$0.353\ 658\ 941 \times 10^{-2}$
500	$0.263\ 889\ 776 \times 10^1$
600	$0.123\ 443\ 146 \times 10^2$

^a It is recommended to verify the programmed equation using 8 byte real values for all three values of T given in this table.

8.2 The Saturation-Temperature Equation (Backward Equation)

The saturation-temperature solution of Eq. (29) reads

$$\frac{T_s}{T^*} = \frac{n_{10} + D - \left[(n_{10} + D)^2 - 4(n_9 + n_{10}D) \right]^{1/2}}{2} \quad (31)$$

where $T^* = 1 \text{ K}$ and

$$D = \frac{2G}{-F - (F^2 - 4EG)^{1/2}}$$

with

$$E = \beta^2 + n_3\beta + n_6$$

$$F = n_1\beta^2 + n_4\beta + n_7$$

$$G = n_2\beta^2 + n_5\beta + n_8$$

and β according to Eq. (29a). The coefficients n_i of Eq. (31) are listed in Table 34.

Range of validity

Equation (31) has the same range of validity as Eq. (30), which means that it covers the vapor-liquid saturation line according to the pressure range

$$611.213 \text{ Pa} \leq p \leq 22.064 \text{ MPa} .$$

The value of 611.213 Pa corresponds to the pressure when Eq. (31) is extrapolated to 273.15 K.

Consistency with the basic equation

Since the saturation-pressure equation, Eq. (30), and the saturation-temperature equation, Eq. (31), have been derived from the same implicit equation, Eq. (29), for describing the saturation line, both Eq. (30) and Eq. (31) are *completely* consistent with each other.

Computer-program verification

To assist the user in computer-program verification of Eq. (31), Table 36 contains test values for three selected pressures.

Table 36. Saturation temperatures calculated from Eq. (31) for selected values of p^a

p/MPa	T_s/K
0.1	$0.372\,755\,919 \times 10^3$
1	$0.453\,035\,632 \times 10^3$
10	$0.584\,149\,488 \times 10^3$

^a It is recommended to verify the programmed equation using 8 byte real values for all three values of p given in this table.

9 Basic Equation for Region 5

This section contains all details relevant for the use of the equations for region 5 of IAPWS-IF97. Information about the consistency at the boundary between regions 2 and 5 is summarized in Section 10. The results of computing-time comparisons between IAPWS-IF97 and IFC-67 are given in Section 11. The estimates of uncertainty of the most relevant properties can be found in Section 12.

The basic equation for this high-temperature region is a fundamental equation for the specific Gibbs free energy g . This equation is expressed in dimensionless form, $\gamma = g/(RT)$, and is separated into two parts, an ideal-gas part γ^o and a residual part γ^r , so that

$$\frac{g(p, T)}{RT} = \gamma(\pi, \tau) = \gamma^o(\pi, \tau) + \gamma^r(\pi, \tau) , \quad (32)$$

where $\pi = p/p^*$ and $\tau = T^*/T$ with R given by Eq. (1).

The equation for the ideal-gas part γ^o of the dimensionless Gibbs free energy reads

$$\gamma^o = \ln \pi + \sum_{i=1}^6 n_i^o \tau^{J_i^o} , \quad (33)$$

where $\pi = p/p^*$ and $\tau = T^*/T$ with $p^* = 1$ MPa and $T^* = 1000$ K. The coefficients n_1^o and n_2^o were adjusted in such a way that the values for the specific internal energy and specific entropy in the ideal-gas state relate to Eq.(8). Table 37 contains the coefficients n_i^o and exponents J_i^o of Eq.(33).

Table 37. Numerical values of the coefficients and exponents of the ideal-gas part γ^o of the dimensionless Gibbs free energy for region 5, Eq. (33)

i	J_i^o	n_i^o	i	J_i^o	n_i^o
1	0	$-0.131\ 799\ 836\ 742\ 01 \times 10^2$	4	-2	$0.369\ 015\ 349\ 803\ 33$
2	1	$0.685\ 408\ 416\ 344\ 34 \times 10^1$	5	-1	$-0.311\ 613\ 182\ 139\ 25 \times 10^1$
3	-3	$-0.248\ 051\ 489\ 334\ 66 \times 10^{-1}$	6	2	$-0.329\ 616\ 265\ 389\ 17$

The form of the residual part γ^r of the dimensionless Gibbs free energy is as follows:

$$\gamma^r = \sum_{i=1}^5 n_i \pi^{I_i} \tau^{J_i} , \quad (34)$$

where $\pi = p/p^*$ and $\tau = T^*/T$ with $p^* = 1$ MPa and $T^* = 1000$ K. The coefficients n_i and exponents I_i and J_i of Eq. (34) are listed in Table 38.

All thermodynamic properties can be derived from Eq.(32) by using the appropriate combinations of the ideal-gas part γ^o , Eq.(33), and the residual part γ^r , Eq.(34), of the dimensionless Gibbs free energy and their derivatives. Relations between the relevant thermodynamic properties and γ^o and γ^r and their derivatives are summarized in Table 39. All required derivatives of the ideal-gas part and of the residual part of the dimensionless Gibbs free energy are explicitly given in Table 40 and Table 41, respectively.

Table 38. Numerical values of the coefficients and exponents of the residual part γ^r of the dimensionless Gibbs free energy for region 5, Eq. (34)

i	I_i	J_i	n_i
1	1	0	$-0.125\ 631\ 835\ 895\ 92 \times 10^{-3}$
2	1	1	$0.217\ 746\ 787\ 145\ 71 \times 10^{-2}$
3	1	3	$-0.459\ 428\ 208\ 999\ 10 \times 10^{-2}$
4	2	9	$-0.397\ 248\ 283\ 595\ 69 \times 10^{-5}$
5	3	3	$0.129\ 192\ 282\ 897\ 84 \times 10^{-6}$

Table 39. Relations of thermodynamic properties to the ideal-gas part γ^o and the residual part γ^r of the dimensionless Gibbs free energy and their derivatives ^a when using Eq. (32)

Property	Relation
Specific volume $v = (\partial g / \partial p)_T$	$v(\pi, \tau) \frac{p}{RT} = \pi(\gamma_\pi^o + \gamma_\pi^r)$
Specific internal energy $u = g - T(\partial g / \partial T)_p - p(\partial g / \partial p)_T$	$\frac{u(\pi, \tau)}{RT} = \tau(\gamma_\tau^o + \gamma_\tau^r) - \pi(\gamma_\pi^o + \gamma_\pi^r)$
Specific entropy $s = -(\partial g / \partial T)_p$	$\frac{s(\pi, \tau)}{R} = \tau(\gamma_\tau^o + \gamma_\tau^r) - (\gamma^o + \gamma^r)$
Specific enthalpy $h = g - T(\partial g / \partial T)_p$	$\frac{h(\pi, \tau)}{RT} = \tau(\gamma_\tau^o + \gamma_\tau^r)$
Specific isobaric heat capacity $c_p = (\partial h / \partial T)_p$	$\frac{c_p(\pi, \tau)}{R} = -\tau^2(\gamma_{\tau\tau}^o + \gamma_{\tau\tau}^r)$
Specific isochoric heat capacity $c_v = (\partial u / \partial T)_v$	$\frac{c_v(\pi, \tau)}{R} = -\tau^2(\gamma_{\tau\tau}^o + \gamma_{\tau\tau}^r) - \frac{(1 + \pi\gamma_\pi^r - \tau\pi\gamma_{\pi\tau}^r)^2}{1 - \pi^2\gamma_{\pi\pi}^r}$
Speed of sound $w = v[-(\partial p / \partial v)_s]^{1/2}$	$\frac{w^2(\pi, \tau)}{RT} = \frac{1 + 2\pi\gamma_\pi^r + \pi^2\gamma_\pi^{r2}}{(1 - \pi^2\gamma_{\pi\pi}^r) + \frac{(1 + \pi\gamma_\pi^r - \tau\pi\gamma_{\pi\tau}^r)^2}{\tau^2(\gamma_{\tau\tau}^o + \gamma_{\tau\tau}^r)}}$

^a $\gamma_\pi^r = \left[\frac{\partial \gamma^r}{\partial \pi} \right]_\tau$, $\gamma_{\pi\pi}^r = \left[\frac{\partial^2 \gamma^r}{\partial \pi^2} \right]_\tau$, $\gamma_\tau^r = \left[\frac{\partial \gamma^r}{\partial \tau} \right]_\pi$, $\gamma_{\tau\tau}^r = \left[\frac{\partial^2 \gamma^r}{\partial \tau^2} \right]_\pi$, $\gamma_{\pi\tau}^r = \left[\frac{\partial^2 \gamma^r}{\partial \pi \partial \tau} \right]$, $\gamma_\tau^o = \left[\frac{\partial \gamma^o}{\partial \tau} \right]_\pi$, $\gamma_{\tau\tau}^o = \left[\frac{\partial^2 \gamma^o}{\partial \tau^2} \right]_\pi$

Table 40. The ideal-gas part γ^o of the dimensionless Gibbs free energy and its derivatives ^a according to Eq. (33)

$$\begin{aligned}\gamma^o &= \ln \pi + \sum_{i=1}^6 n_i^o \tau^{J_i^o} \\ \gamma_\pi^o &= 1/\pi + 0 \\ \gamma_{\pi\pi}^o &= -1/\pi^2 + 0 \\ \gamma_\tau^o &= 0 + \sum_{i=1}^6 n_i^o J_i^o \tau^{J_i^o-1} \\ \gamma_{\tau\tau}^o &= 0 + \sum_{i=1}^6 n_i^o J_i^o (J_i^o - 1) \tau^{J_i^o-2} \\ \gamma_{\pi\tau}^o &= 0 + 0\end{aligned}$$

$${}^a \gamma_\pi^o = \left[\frac{\partial \gamma^o}{\partial \pi} \right]_\tau, \gamma_{\pi\pi}^o = \left[\frac{\partial^2 \gamma^o}{\partial \pi^2} \right]_\tau, \gamma_\tau^o = \left[\frac{\partial \gamma^o}{\partial \tau} \right]_\pi, \gamma_{\tau\tau}^o = \left[\frac{\partial^2 \gamma^o}{\partial \tau^2} \right]_\pi, \gamma_{\pi\tau}^o = \left[\frac{\partial^2 \gamma^o}{\partial \pi \partial \tau} \right]$$

Table 41. The residual part γ^r of the dimensionless Gibbs free energy and its derivatives ^a according to Eq. (34)

$$\begin{aligned}\gamma^r &= \sum_{i=1}^5 n_i \pi^{I_i} \tau^{J_i} \\ \gamma_\pi^r &= \sum_{i=1}^5 n_i I_i \pi^{I_i-1} \tau^{J_i} & \gamma_{\pi\pi}^r &= \sum_{i=1}^5 n_i I_i (I_i - 1) \pi^{I_i-2} \tau^{J_i} \\ \gamma_\tau^r &= \sum_{i=1}^5 n_i \pi^{I_i} J_i \tau^{J_i-1} & \gamma_{\tau\tau}^r &= \sum_{i=1}^5 n_i \pi^{I_i} J_i (J_i - 1) \tau^{J_i-2} \\ \gamma_{\pi\tau}^r &= \sum_{i=1}^5 n_i I_i \pi^{I_i-1} J_i \tau^{J_i-1}\end{aligned}$$

$${}^a \gamma_\pi^r = \left[\frac{\partial \gamma^r}{\partial \pi} \right]_\tau, \gamma_{\pi\pi}^r = \left[\frac{\partial^2 \gamma^r}{\partial \pi^2} \right]_\tau, \gamma_\tau^r = \left[\frac{\partial \gamma^r}{\partial \tau} \right]_\pi, \gamma_{\tau\tau}^r = \left[\frac{\partial^2 \gamma^r}{\partial \tau^2} \right]_\pi, \gamma_{\pi\tau}^r = \left[\frac{\partial^2 \gamma^r}{\partial \pi \partial \tau} \right]$$

Range of validity

Equation (32) covers region 5 of IAPWS-IF97 defined by the following temperature and pressure range:

$$1073.15 \text{ K} \leq T \leq 2273.15 \text{ K} \quad 0 < p \leq 10 \text{ MPa} .$$

In this range Eq. (32) is only valid for pure undissociated water, any dissociation will have to be taken into account separately.

Computer-program verification

To assist the user in computer-program verification of Eq. (32), Table 42 contains test values of the most relevant properties.

Table 42. Thermodynamic property values calculated from Eq. (32) for selected values of T and p ^a

	$T = 1500 \text{ K},$ $p = 0.5 \text{ MPa}$	$T = 1500 \text{ K},$ $p = 8 \text{ MPa}$	$T = 2000 \text{ K},$ $p = 8 \text{ MPa}$
$v/(\text{m}^3 \text{ kg}^{-1})$	$0.138\,455\,354 \times 10^1$	$0.865\,156\,616 \times 10^{-1}$	$0.115\,743\,146$
$h/(\text{kJ kg}^{-1})$	$0.521\,976\,332 \times 10^4$	$0.520\,609\,634 \times 10^4$	$0.658\,380\,291 \times 10^4$
$u/(\text{kJ kg}^{-1})$	$0.452\,748\,654 \times 10^4$	$0.451\,397\,105 \times 10^4$	$0.565\,785\,774 \times 10^4$
$s/(\text{kJ kg}^{-1} \text{ K}^{-1})$	$0.965\,408\,431 \times 10^1$	$0.836\,546\,724 \times 10^1$	$0.915\,671\,044 \times 10^1$
$c_p/(\text{kJ kg}^{-1} \text{ K}^{-1})$	$0.261\,610\,228 \times 10^1$	$0.264\,453\,866 \times 10^1$	$0.285\,306\,750 \times 10^1$
$w/(\text{m s}^{-1})$	$0.917\,071\,933 \times 10^3$	$0.919\,708\,859 \times 10^3$	$0.105\,435\,806 \times 10^4$

^a It is recommended to verify programmed functions using 8 byte real values for all three combinations of T and p given in this table.

10 Consistency at Region Boundaries

For any calculation of thermodynamic properties of water and steam across the region boundaries, the equations of IAPWS-IF97 have to be sufficiently consistent along the corresponding boundary. For the properties considered in this respect, this section presents the achieved consistencies in comparison to the permitted inconsistencies according to the so-called Prague values [13].

10.1 Consistency at Boundaries between Single-Phase Regions

For the boundaries between single-phase regions the consistency investigations were performed for the following basic equations and region boundaries; see Fig. 1:

- Equations (7) and (28) along the 623.15 K isotherm for pressures from 16.53 MPa (p_s from Eq. (30) for 623.15 K) to 100 MPa corresponding to the boundary between regions 1 and 3.

- Equations (15) and (28) with respect to the boundary between regions 2 and 3 defined by the B23-equation, Eq. (5), for temperatures between 623.15 K and 863.15 K.
- Equations (15) and (32) with respect to the 1073.15 K isotherm for $p \leq 10$ MPa corresponding to the boundary between regions 2 and 5.

The results of the consistency investigations for these three region boundaries are summarized in Table 43. In addition to the permitted inconsistencies corresponding to the Prague values [13], the actual inconsistencies characterized by their maximum and root-mean-square values, $|\Delta x|_{\max}$ and Δx_{RMS} , along the three boundaries are given for $x = v, h, c_p, s, g,$ and w . It can be seen that the inconsistencies between the basic equations along the corresponding region boundaries are extremely small.

Table 43. Inconsistencies between basic equations for single-phase regions at the joint region boundary

Inconsistency Δx	Prague value	Regions 1/3 Eqs. (7)/(28)		Regions 2/3 Eqs. (15)/(28)		Regions 2/5 Eqs. (15)/(32)	
		$ \Delta x _{\max}$	Δx_{RMS}^a	$ \Delta x _{\max}$	Δx_{RMS}^a	$ \Delta x _{\max}$	Δx_{RMS}^a
$ \Delta v /\%$	0.05	0.004	0.002	0.018	0.007	0.002	0.001
$ \Delta h /(\text{kJ kg}^{-1})$	0.2	0.031	0.014	0.134	0.073	0.020	0.012
$ \Delta c_p /\%$	1	0.195	0.058	0.353	0.169	0.081	0.048
$ \Delta s /(\text{J kg}^{-1} \text{K}^{-1})$	0.2	0.042	0.022	0.177	0.094	0.042	0.025
$ \Delta g /(\text{kJ kg}^{-1})$	0.2	0.005	0.005	0.005	0.003	0.026	0.021
$ \Delta w /\%$	1 ^b	0.299	0.087	0.403	0.073	0.021	0.009

^a The Δx_{RMS} values (see Nomenclature) were calculated from about 10 000 points evenly distributed along the corresponding boundary.

^b The permitted inconsistency value for w is not included in the Prague values.

10.2 Consistency at the Saturation Line

The consistency investigations along the vapor-liquid saturation line were performed for the properties $p_s, T_s,$ and g . The calculations concern the following basic equations and ranges of the saturation line, see Fig. 1; the way of calculating the inconsistencies $\Delta p_s, \Delta T_s,$ and Δg is also given:

- Equations (7), (15) and (30) on the saturation line for temperatures from $T_t = 273.15$ K to 623.15 K.

$$\Delta p_s = p_{s, \text{Eq.(7), Eq.(15)}} - p_{s, \text{Eq.(30)}} \quad (35a)$$

$$\Delta T_s = T_{s, \text{Eq.(7), Eq.(15)}} - T_{s, \text{Eq.(31)}} \quad (35b)$$

$$\Delta g = g_{\text{Eq.(7)}} - g_{\text{Eq.(15)}} \quad (35c)$$

The calculation of p_s and of T_s from Eqs. (7) and (15) is made via the Maxwell criterion (phase-equilibrium condition) for given values of T or p . The g values are determined for given T values and corresponding p_s values from Eq. (30).

- Equations (28) and (30) on the saturation line for temperatures from 623.15 K to $T_c = 647.096$ K.

$$\Delta p_s = p_{s, \text{Eq.(28)}} - p_{s, \text{Eq.(30)}} \quad (36a)$$

$$\Delta T_s = T_{s, \text{Eq.(28)}} - T_{s, \text{Eq.(31)}} \quad (36b)$$

$$\Delta g = g'_{\text{Eq.(28), Eq.(30)}} - g''_{\text{Eq.(28), Eq.(30)}} \quad (36c)$$

The calculation of p_s and T_s from Eq. (28) is made via the Maxwell criterion for given temperatures or pressures, respectively. The inconsistency Δg corresponds to the difference $g'(\rho', T) - g''(\rho'', T)$ which is calculated from Eq. (28) after ρ' and ρ'' are determined from Eq. (28) by iteration for given T values and corresponding p_s values from Eq. (30).

- Equations (7), (15) and (28) on the saturation line at 623.15 K. This is the only point on the saturation line where the validity ranges of the fundamental equations of regions 1 to 3 meet each other.

$$\Delta p_s = p_{s, \text{Eq.(7), Eq.(15)}} - p_{s, \text{Eq.(28)}} \quad (37a)$$

$$\Delta T_s = T_{s, \text{Eq.(7), Eq.(15)}} - T_{s, \text{Eq.(28)}} \quad (37b)$$

$$\Delta g = g_{\text{Eq.(7), Eq.(15)}} - g_{\text{Eq.(28)}} \quad (37c)$$

All three properties p_s and T_s and g are calculated via the Maxwell criterion from the corresponding equations.

The results of these consistency investigations along the saturation line are summarized in Table 44. In addition to the permitted inconsistencies corresponding to the Prague values [13], the actual inconsistencies characterized by their maximum and root-mean-square values, $|\Delta x|_{\max}$ and Δx_{RMS} , for the two sections of the saturation line are given for $x = p_s, T_s$ and g . It can be seen that the inconsistencies between the basic equations for the corresponding single-phase region and the saturation-pressure equation are extremely small. This statement also holds for the fundamental equations, Eqs. (7), (15), and (28), among one another and not only in relation to the saturation-pressure equation, Eq. (30), see the last column in Table 44.

Table 44. Inconsistencies between the basic equations valid at the saturation line

Inconsistency Δx	Prague value	$T_t \leq T \leq 623.15 \text{ K}$ Eqs. (7),(15)/(30)		$623.15 \text{ K} \leq T \leq T_c$ Eqs. (28)/(30)		$T = 623.15 \text{ K}$ Eqs. (7),(15)/(28)
		$ \Delta x _{\max}$	Δx_{RMS}^a	$ \Delta x _{\max}$	Δx_{RMS}^a	
$ \Delta p_s /\%$	0.05	0.0069	0.0033	0.0026	0.0015	0.0041
$ \Delta T_s /\%$	0.02	0.0006	0.0003	0.0003	0.0002	0.0006
$ \Delta g /(\text{kJ kg}^{-1})$	0.2	0.012	0.006	0.002	0.001	0.005

^a The Δx_{RMS} values (see Nomenclature) were calculated from about 3000 points evenly distributed along the two sections of the saturation line.

11 Computing Time of IAPWS-IF97 in Relation to IFC-67

A very important requirement for IAPWS-IF97 was that its computing speed in relation to IFC-67 should be significantly faster. The computation-speed investigations of IAPWS-IF97 in comparison with IFC-67 are based on a special procedure agreed to IAPWS.

The computing times were measured with a benchmark program developed by IAPWS; this program calculates the corresponding functions at a large number of state points well distributed proportionately over each region. The test configuration agreed on was a PC Intel 486 DX 33 processor and the MS Fortran 5.1 compiler. The relevant functions of IAPWS-IF97 were programmed with regard to short computing times. The calculations with IFC-67 were carried out with the ASME program package [14] speeded up by excluding all parts which were not needed for these special benchmark tests.

The measured computing times were used to calculate computing-time ratios IFC-67/IAPWS-IF97, called CTR values in the following. These CTR values, determined in a different way for regions 1, 2, and 4 (see Section 11.1) and for regions 3 and 5 (see Section 11.2), are the characteristic quantities for the judgment of how much faster the calculations with IAPWS-IF97 are in comparison with IFC-67. Metastable states are not included in these investigations.

11.1 Computing-Time Investigations for Regions 1, 2, and 4

The computing-time investigations for regions 1, 2, and 4, which are particularly relevant to computing time, were performed for the functions listed in Table 45. Each function is associated with a frequency-of-use value. Both the selection of the functions and the values for the corresponding frequency of use are based on a worldwide survey made among the power plant companies and related industries.

For the computing-time comparison between IAPWS-IF97 and IFC-67 for regions 1, 2, and 4, the *total* CTR value of these three regions together was the decisive criterion, where the

frequencies of use have to be taken into account. The total CTR value was calculated as follows: As has been described before, the computing times for each function were determined for IFC-67 and for IAPWS-IF97. Then, these values were weighted by the corresponding frequencies of use and added up for the 16 functions of the three regions. The total CTR value is obtained from the sum of the weighted computing times for IFC-67 divided by the corresponding value for IAPWS-IF97. The total CTR value for regions 1, 2, and 4 amounts to

$$\text{CTR}_{\text{regions 1,2,4}} = 5.1 . \quad (38)$$

This means that for regions 1, 2, and 4 together the property calculations with IAPWS-IF97 are more than five times faster than with IFC-67.

Table 45. Results of the computing-time investigations of IAPWS-IF97 in relation to IFC-67 for regions 1, 2, and 4^a

Region ^b	Function	Frequency of use %	Computing-time ratio IFC-67 / IF97
1	$v(p, T)$	2.9	2.7
	$h(p, T)$	9.7	2.9
	$T(p, h)$	3.5	24.8
	$h(p, s)$	1.2	10.0
Σ region 1:			5.6 ^c
2	$v(p, T)$	6.1	2.1
	$h(p, T)$	12.1	2.9
	$s(p, T)$	1.4	1.4
	$T(p, h)$	8.5	12.4
	$v(p, h)$	3.1	6.4
	$s(p, h)$	1.7	4.2
	$T(p, s)$	1.7	8.1
	$h(p, s)$	4.9	5.6
Σ region 2:			5.0 ^c
4	$p_s(T)$	8.0	1.7
	$T_s(p)$	30.7	5.6
	$h'(p)$	2.25	4.4
	$h''(p)$	2.25	4.2
Σ region 4:			4.9 ^c
Σ regions 1, 2 and 4:			5.1^c

^a Based on the agreed PC Intel 486 DX 33 with MS Fortran 5.1 compiler.

^b For the definition of the regions see Fig. 1.

^c This CTR value is based on the computing times for the single functions weighted by the frequency-of-use values; see text.

Table 45 also contains total CTR values separately for each of regions 1, 2, and 4. In addition, CTR values for each single function are given. When using IAPWS-IF97 the functions depending on p, h and p, s for regions 1 and 2 and on p for region 4 were calculated from the backward equations alone (functions explicit in T) or from the basic equations in combination with the corresponding backward equation.

If a faster processor than specified above is used for the described benchmark tests, similar CTR values are obtained. A corresponding statement is also valid for other compilers than the specified one.

11.2 Computing-Time Investigations for Regions 3 and 5

For regions 3 and 5 the CTR values only relate to single functions and are given by the quotient of the computing time needed for IFC-67 calculation and the computing time when using IAPWS-IF97; there are no frequency-of-use values for functions relevant to these two regions.

For region 3 of IAPWS-IF97, corresponding to regions 3 and 4 of IFC-67, the computing-time investigations relate to the functions $p(v, T)$, $h(v, T)$, $c_p(v, T)$, and $s(v, T)$ where 10 % of the test points are in region 4 of IFC-67. For region 5 of IAPWS-IF97, the computing-time investigations relate only to the functions $v(p, T)$, $h(p, T)$, and $c_p(p, T)$, where the CTR values were determined for 1073.15 K, the maximum temperature for which IFC-67 is valid.

Table 46 lists the CTR values obtained for the relevant functions of regions 3 and 5. Roughly speaking, IAPWS-IF97 is more than three times faster than IFC-67 for region 3 and more than nine times faster for the 1073.15 K isotherm where region 5 overlaps IFC-67.

Table 46. Results of the computing-time investigations of IAPWS-IF97 in relation to IFC-67 for regions 3 and 5^a

Region ^b	Function	Computing time ratio IFC-67/IF97
3	$p(v, T)$	3.8
	$h(v, T)$	4.3
	$c_p(v, T)$	2.9
	$s(v, T)$	3.2
5	$v(p, T)$	8.9 ^c
	$h(p, T)$	11.9 ^c
	$c_p(p, T)$	15.8 ^c

^a Based on the agreed PC Intel 486 DX 33 with MS Fortran 5.1 compiler.

^b For the definition of the regions see Fig. 1.

^c Determined for the 1073.15 K isotherm for which IFC-67 is valid.

12 Estimates of Uncertainties

Estimates have been made of the uncertainty of the specific volume, specific isobaric heat capacity, speed of sound, and saturation pressure when calculated from the corresponding equations of IAPWS-IF97. These estimates were derived from the uncertainties of IAPWS-95 [3], from which the input values for fitting the IAPWS-IF97 equations were calculated, and in addition by taking into account the deviations between the corresponding values calculated from IAPWS-IF97 and IAPWS-95. Since there is no reasonable basis for estimating the uncertainty of specific enthalpy (because specific enthalpy is dependent on the selection of the zero point, only enthalpy differences of different size are of interest), no uncertainty is given for this property. However, the uncertainty of isobaric enthalpy differences is smaller than the uncertainty in the isobaric heat capacity.

For the single-phase region, tolerances are indicated in Figs. 3 to 5 which give the estimated uncertainties in various areas. As used here "tolerance" means the range of possible values as judged by IAPWS, and no statistical significance can be attached to it. With regard to the uncertainty for the speed of sound and the specific isobaric heat capacity, see Figs. 4 and 5, it should be noted that the uncertainties for these properties increase drastically when approaching the critical point. The statement "no definitive uncertainty estimates possible" for temperatures above 1273 K is based on the fact that this range is beyond the range of validity of IAPWS-95 and the corresponding input values for IAPWS-IF97 were extrapolated from IAPWS-95. From various tests of IAPWS-95 [3] it is expected that these extrapolations yield reasonable values.

For the saturation pressure, the estimate of uncertainty is shown in Fig. 6.

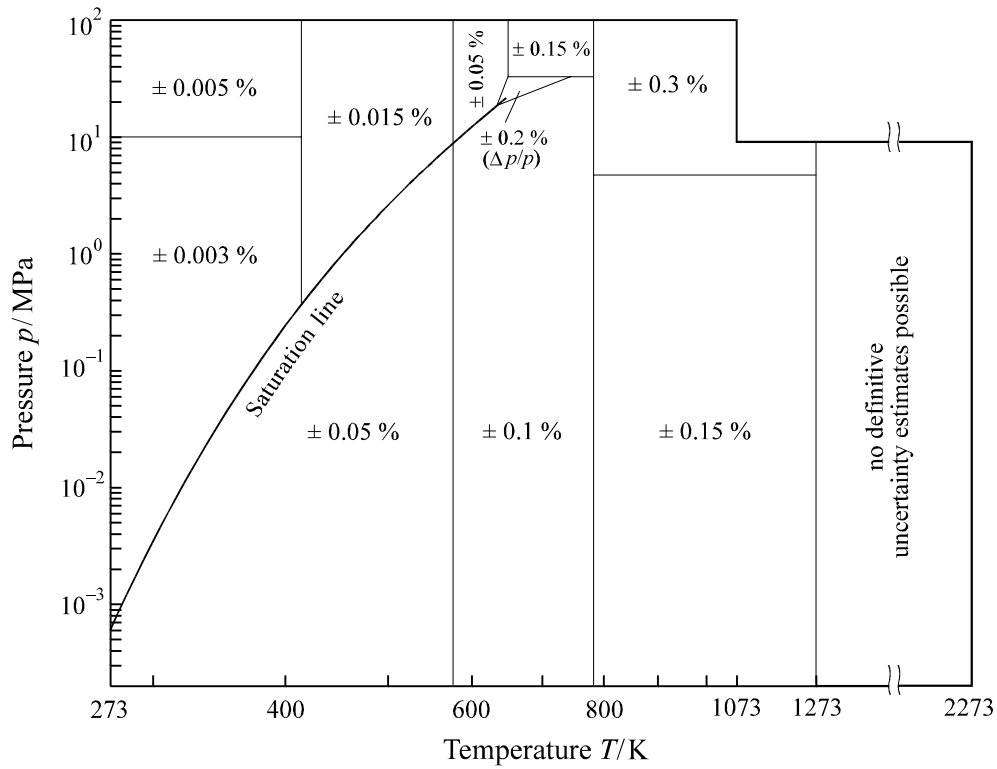


Fig. 3. Uncertainties in specific volume, $\Delta v/v$, estimated for the corresponding equations of IAPWS-IF97. In the enlarged critical region (triangle), the uncertainty is given as percentage uncertainty in pressure, $\Delta p/p$. This region is bordered by the two isochores $0.0019 \text{ m}^3 \text{ kg}^{-1}$ and $0.0069 \text{ m}^3 \text{ kg}^{-1}$ and by the 30 MPa isobar. The positions of the lines separating the uncertainty regions are approximate.

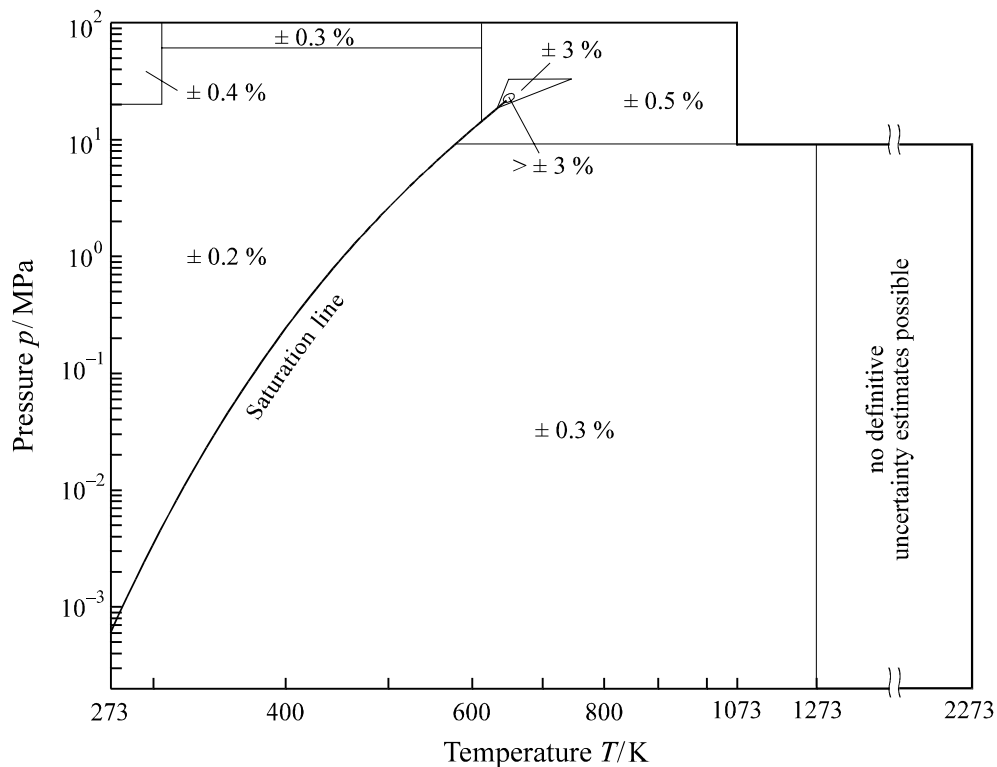


Fig. 4. Uncertainties in specific isobaric heat capacity, $\Delta c_p/c_p$, estimated for the corresponding equations of IAPWS-IF97. For the definition of the triangle around the critical point, see Fig. 3. The positions of the lines separating the uncertainty regions are approximate.

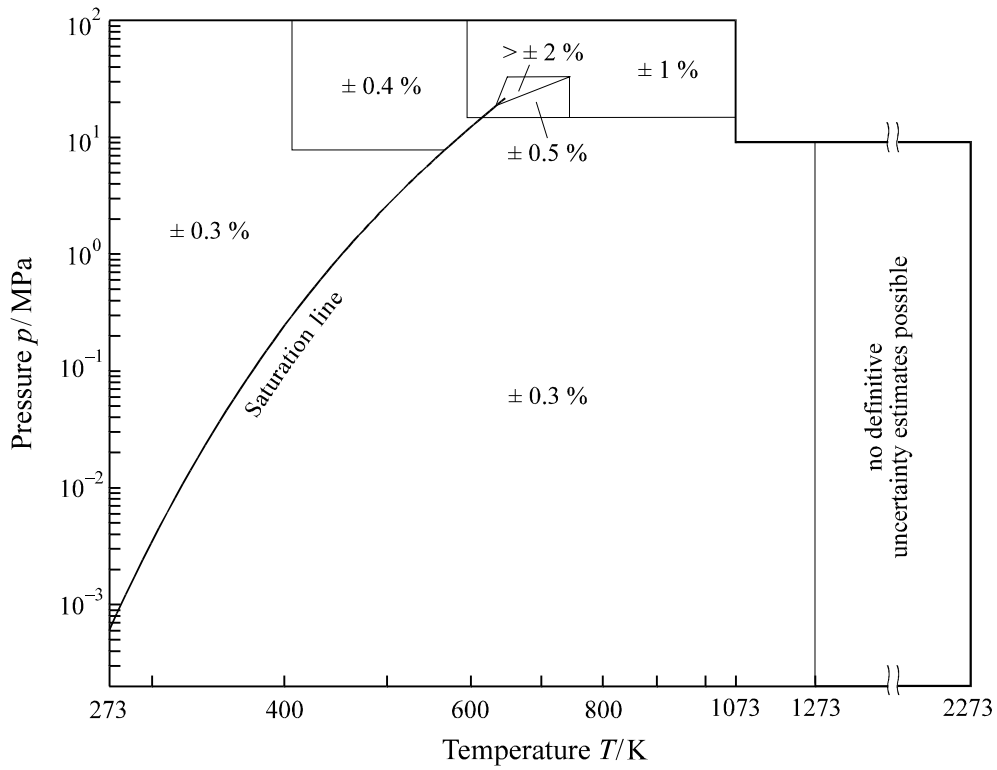


Fig. 5. Uncertainties in speed of sound, $\Delta w/w$, estimated for the corresponding equations of IAPWS-IF97. For the definition of the triangle around the critical point, see Fig. 3. The positions of the lines separating the uncertainty regions are approximate.

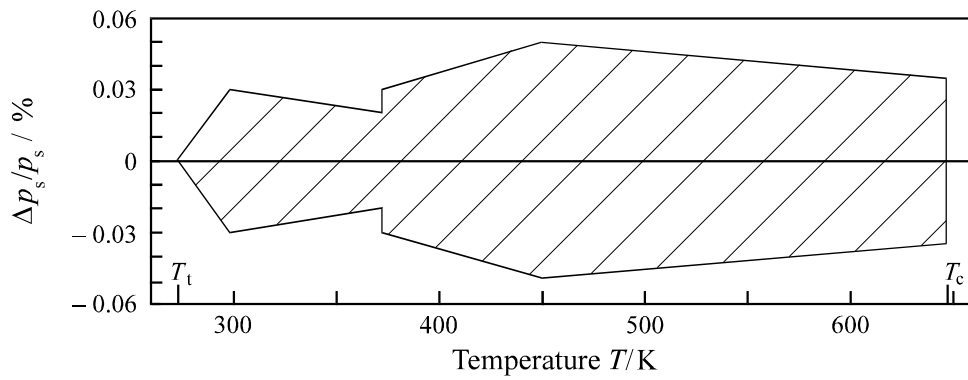


Fig. 6. Uncertainties in saturation pressure, $\Delta p_s/p_s$, estimated for the saturation-pressure equation, Eq. (30).

13 References

- [1] International Formulation Committee of the 6th International Conference on the Properties of Steam, *The 1967 IFC Formulation for Industrial Use*, Verein Deutscher Ingenieure, Düsseldorf, 1967.
- [2] Wagner, W., Cooper, J. R., Dittmann, A., Kijima, J., Kretzschmar, H.-J., Kruse, A., Mareš, R., Oguchi, K., Sato, H., Stöcker, I., Šifner, O., Takaishi, Y., Tanishita, I., Trübenbach, J., and Willkommen, Th., *The IAPWS Industrial Formulation 1997 for the Thermodynamic Properties of Water and Steam*, to be submitted for publication.
- [3] IAPWS Release on the *IAPWS Formulation 1995 for the Thermodynamic Properties of Ordinary Water Substance for General and Scientific Use*, IAPWS Secretariat 1996.
- [4] Cohen, E. R. and Taylor, B. N., *The 1986 Adjustment of the Fundamental Physical Constants*, CODATA Bulletin No. 63, Committee on Data for Science and Technology, Int. Council of Scientific Unions, Pergamon Press, Oxford, 1986.
- [5] Audi, G. and Wapstra, A. H., The 1993 atomic mass evaluation, (I) Atomic mass table, *Nuclear Physics A* 565 (1993), 1-65.
- [6] IUPAC Commission on the Atomic Weights and Isotopic Abundances, Subcommittee for Isotopic Abundance Measurements, Isotopic compositions of the elements 1989, *Pure and Appl. Chem.* 63 (1991), 991-1002.
- [7] IAPWS Release on the *Values of Temperature, Pressure and Density of Ordinary and Heavy Water Substances at Their Respective Critical Points*, in *Physical Chemistry of Aqueous Systems: Meeting the Needs of Industry*, edited by H. J. White, Jr. et al., Proceedings of the 12th International Conference on the Properties of Water and Steam, pp. A 101 - A 102, Begell House, New York, 1995.
- [8] Preston-Thomas, H., The International Temperature Scale of 1990 (ITS-90), *Metrologia* 27 (1990), 3-10.
- [9] Guildner, L. A., Johnson, D. P., and Jones, F. E., Vapor Pressure of Water at Its Triple Point, *J. Res. Natl. Bur. Stand.* 80A (1976), 505-521.
- [10] IAPWS Release on the *Pressure along the Melting and Sublimation Curves of Ordinary Water Substance*, in Wagner, W., Saul, A., and Pruß, A., *J. Phys. Chem. Ref. Data* 23, 515-527 (1994), also in *Physical Chemistry of Aqueous Systems: Meeting the Needs of Industry*, edited by H. White, Jr. et al., Proceedings of the 12th International Conference on the Properties of Water and Steam, pp. A 9 - A 12, Begell House, New York, 1995.
- [11] Pruß, A. and Wagner, W., *New International Formulation for the Thermodynamic Properties of Ordinary Water Substance for General and Scientific Use*, to be submitted to *J. Phys. Chem. Ref. Data* (1997).
- [12] IAPWS Supplementary Release on *Saturation Properties of Ordinary Water Substance*, in Wagner, W. and Pruß, A., *J. Phys. Chem. Ref. Data* 22, 783-787 (1993), also in *Physical Chemistry of Aqueous Systems: Meeting the Needs of Industry*, edited by H. White, Jr. et al., Proceedings of the 12th International Conference on the Properties of Water and Steam, pp. A 143-A 149, Begell House, New York, 1995.
- [13] Minutes of the meetings of the International Formulation Committee of ICPS in Prague, 1965.
- [14] McClintock, R. B. and Silvestri, G. J., *Formulations and iterative procedures for the calculation of properties of steam*, The American Society of Mechanical Engineers, New York, 1968.